Optical and Visual Performance in Typically-sighted and Highly Aberrated Eyes

by

Sujata Rijal

A dissertation submitted to the

Physiological Optics and Vision Sciences Graduate Program

College of Optometry

in partial fulfillment of the requirements for the degree of

DOCTOR OF PHILOSOPHY

in

Physiological Optics and Vision Science

Chair of Committee: Jason D. Marsack, Ph.D.

Committee Member: Daniel R. Coates Ph.D.

Committee Member: Han Cheng, O.D., Ph.D.

Committee Member: Fuensanta Vera-Diaz, O.D., Ph.D.

University of Houston

August 2021

DEDICATION

"To my grandmothers for their faith in educating girls, in loving memory."

ACKNOWLEDGEMENTS

I would like to acknowledge the contributions and thank the people without whom this dissertation would not have been completed. First, I would like to thank my advisor Dr. Jason Marsack for all his support and guidance throughout my Ph.D. journey both personally and professionally. The flexibility I received to work at my own pace, choose all my projects, work in collaboration with other labs and be involved in all the aspects of the project administration under his guidance has contributed immensely to my growth as a budding researcher. I am also deeply influenced by his kind and very considerate personality which has only made me a better individual.

I would like to thank my dissertation committee members for their collaboration, valuable feedback and suggestions. Thank you, Dr. Daniel Coates for your time, support and letting me use the resources in your lab for the reading study. I am truly grateful for all of our readings and discussions, which have contributed to my understanding of visual psychophysics. I would like to thank Dr. Han Cheng for the collaboration in the CamBlobs2 study and all her feedback on the manuscript that has strengthened the importance of the findings presented. As her TA, she provided me with advice that has contributed greatly to my personal growth. Thank you, Dr. Fuensanta Vera-Diaz for being very welcoming, giving me a tour of the lab at NECO in the middle of a pandemic and providing me your valuable feedback as an external committee member.

I would like to thank Dr. Frishman for her excellent leadership which has made the graduate program very systematic. I am very grateful for all the advising sessions and personal suggestions I have received to fulfill the milestones necessary to graduate and for the next step following graduation. I would like to thank Dr. Applegate for all the readings and suggestions which have contributed significantly to my understanding of visual optics.

I would also like to thank past and present members of both the Visual Optics Institute and the Coates Lab: Particularly, I would like to thank Dr. David Rio, Dr. Gareth Hastings, Chi Nguyen, Krish Prahalad and Danny Lew for all the help I received in my projects. Besides the people mentioned, Dr. Matthew Kauffman, and Dr. Sarah Wilting are co-authors on portions of the published work that is presented here. Dr. Ayeswarya Ravikumar, Hope Queener, Dr. Larry Thibos, Dr. Ed and Ms. Charlene Sarver and Dr. John Robson also made significant contributions. I would also like to thank Renee Armacost for making all the administrative work at UHCO very easy to navigate.

I stand on the goodwill and love of my amazing parents: Tara Nath and Devi Maya Rijal; Raj Kumar and Sita Basnet, and support of my wonderful siblings. Thank you, Sudan, my better half for being my mentor and my best friend. Thank you for filling my life with love, laughter, positivity, and knowledge, all in abundance. Thank you Dr. Ashutosh Jnawali for being my student mentor at UHCO, an elder brother, a dear friend and thank you for always opening doors for me. I would also like to thank my friends, especially Apoorva, Angie, Chuan and Erin in the program for helping me adjust to a completely new country. I would like to thank two of my dearest friends outside school, Swati and Bikrant for more than a decade long friendship, many

transferable research skills I have learnt from their respective scientific fields and kindly hosting me many times during these five years whenever I needed a break.

I would like to thank all of the graduate faculty for their classes. I would also like to thank all the subjects for their participation in the research and the clinicians in The Cornea and Contact Lens Service at the University Eye Institute for subject referrals. I acknowledge the research funds that supported the research projects – NIH/NEI R01EY019105 to JDM and RAA, UHCO sVRSG to SR and NIH Core Grant P30EY07551 to UHCO. I acknowledge the journal Optometry and Vision Science and Ophthalmic and Physiological Optics, where chapters 2 and 4 of this dissertation were published, respectively.

GENERAL ABSTRACT

Purpose: This dissertation explores the manner in which typically-sighted individuals and individuals with keratoconus perform simulated, clinical and real-world visual tasks under varying levels uncorrected optical aberration.

Methods: Study 1 tested the viability of a common (rather than an eye-specific) decentration rule for placement of wavefront-guided optics in a wavefront-guided scleral lens. Study 2 quantified threshold word acuity with and without accompanying flanking words at high (100%) and low (25%) contrast over 5 stimulus durations for habitually corrected individuals with keratoconus and typically-sighted individuals. Study 3 quantified the limits of agreement and intra-visit repeatability of the CamBlobs2 contrast sensitivity test and compared the results to the near Pelli-Robson contrast sensitivity test in individuals with keratoconus and typically-sighted individuals.

Results: Study 1 demonstrated that decentering the wavefront-guided correction from the subject-specific location was predicted to lead to an appreciable increase in residual aberration and reduction in visual image quality. Study 2 demonstrated that there was a trend toward elevated threshold word acuity, when compared to visual acuity (which was more pronounced with near low contrast words). Study 3 demonstrated that in typically-sighted individuals, repeatability of both tests was within ± 0.20 logCS and the limit of agreement between near Pelli-Robson and CamBlobs2 scores was -0.08 ± 0.08 for right eyes and -0.05 ± 0.10 logCS for left eyes. The repeatability worsened to ± 0.30 logCS and the limit of agreement between near Pelli-Robson and CamBlobs2 scores was -0.05 ± 0.14 for the keratoconus group.

Conclusions: The wavefront-guided correction must be placed at an eye-specific location to avoid reduction in optical and visual performance predicted to be noticeable to an individual. Larger font sizes are required for word recognition (especially low contrast words) than would be expected from common measurement of high contrast distance visual acuity. Both contrast sensitivity tests were repeatable and with a 0.05 correction, the CamBlobs2 scores showed an excellent agreement with those of the near Pelli-Robson contrast sensitivity test.

TABLE OF CONTENTS

LIST OF TABLES

LIST OF FIGURES

ABBREVIATIONS

ADL	Average decentered location
AMD	Age related macular degeneration
CLEK	Collaborative longitudinal evaluation of keratoconus
CS	Contrast sensitivity
CSF	Contrast sensitivity function
GC	Geometric center
HC	High contrast
HORMS	Higher-order root mean square
LC	Low contrast
LCD	Liquid crystal display
PSF	Point spread function
RMS	Root mean square
SPGD	Stochastic parallel gradient descent
SQuAD	Stanford question answering dataset
VA	Visual acuity
VSX	Visual strehl ratio
WGC	Wavefront-guided correction

1 Chapter 1: Introduction

1.1 Optical performance of the eye

The cornea and crystalline lens are the major refracting components of the eye. As a result of the difference in refractive index between air and cornea (tear film), 2/3 of the refracting power of the ocular surface occurs at the air/tear interface and the remaining 1/3 is contributed by the posterior cornea and crystalline lens. An ideal relationship of the optical surfaces and axial length of the eye (known as emmetropia) results in light from optical infinity coming to a focus on the retina to form a clear image.

1.2 Refractive error

Conditions where the refracting power of the eye and the eye's axial length are not well-matched (known collectively as refractive errors, or ametropias) result in light from infinity not being well-focused on the retina, and the resulting retinal image is blurry. If the eye is too long/short, or the corneal power is too strong/weak, the retinal image will be blurred. If rays from optical infinity are focused in front of the retina, the refractive error is referred to as myopia. If the rays are focused behind the retina, the refractive error is referred to as hyperopia. Refractive error can become more complicated when the level of refractive error is not uniform over all meridians. In the typical eye, this asymmetry in refracting power manifests as sphero-cylindrical refractive errors.

Glasses and contact lenses are commonly used to correct the refractive errors present in the eye. This works well in the typical eye, where sphere and cylindrical errors dominate. However, these are not the only refractive error (aberrations) present in the eye. There are several diseases and optical conditions that lead to increased complexity of the refractive errors of the eye. For instance corneal ectasias like keratoconus[1] have rotationally asymmetric power profiles. Based

on the severity and progression of the conditions, the cornea (kerato) changes from its normal shape to a more conical (conus) in shape. With these types of conditions, there is an increased presence of sphere and cylinder, or lower-order aberrations, as well as higher-order aberrations.[2] Glasses and conventional contact lenses are not capable of fully correcting higher-order aberrations that manifest in eyes with corneal ectasia.[3–7]

1.3 Aberrations (Zernike polynomial, wavefront sensing, aberrations in typical eyes and eyes with keratoconus)

Wavefront sensing is a technique whereby an optical instrument (known as a wavefront sensor or aberrometer) is used to measure the wavefront error (difference between an ideal wavefront that would result in a focused image on the retina, and the actual measured wavefront) of an eye. There are many different forms of wavefront sensing used in clinical practice, with the Shack-Hartmann wavefront sensing being the most common type. The COAS-HD wavefront sensor (Johnson and Johnson Vision, Santa Ana, CA) is an example of a Shack-Hartmann wavefront sensor that is used in both research and clinical settings. In brief, a Shack-Hartmann wavefront sensor sends a low intensity, narrow laser beam through the optics of the eye onto the retina. The light that interacts with the retina then acts as a new point source, resulting in a wavefront that propagates out of the eye through the eye's pupil. The wavefront emerging from the pupil is imaged through a series of relay lenses in the wavefront sensor and projected onto a specialized optic known as a lenslet array, which optically sections the wavefront. This results in a spot field (delimited by the diameter of the pupil) falling onto an imaging device (in the case of the COAS-HD, a CCD camera) located at the focal point of the lenslet array. Figure 1.1 represents an example of a spot pattern and a measured wavefront for a typical eye and highly aberrated eye.

Typically-sighted eye

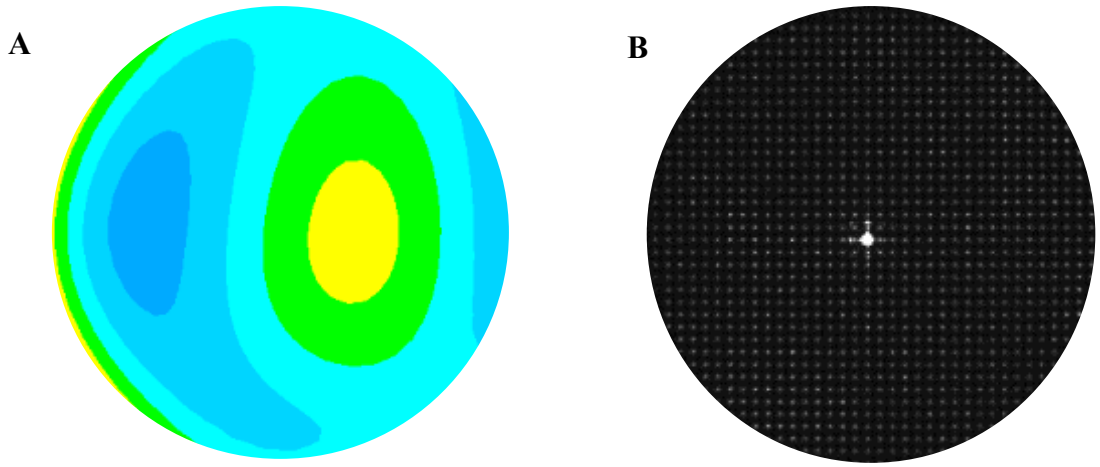

Highly aberrated eye

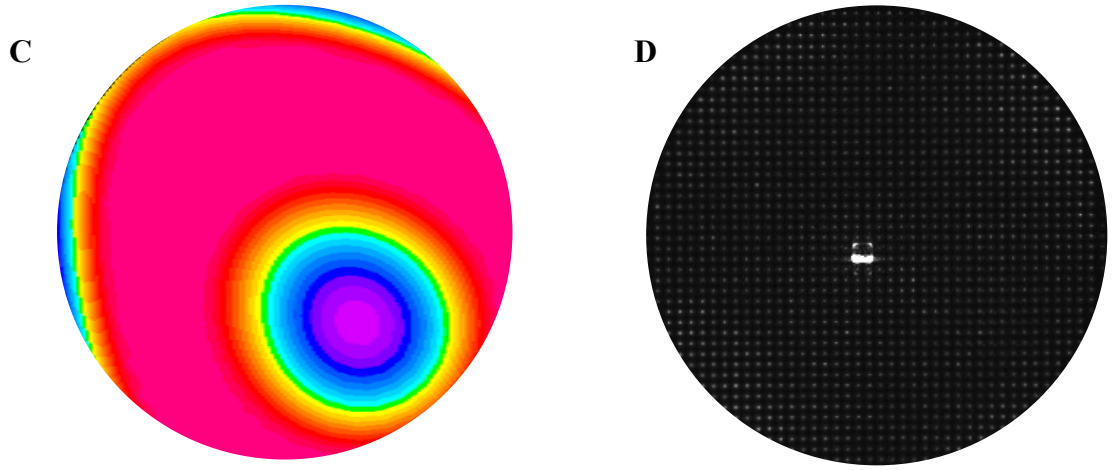

Figure 1.1 An example of a typically-sighted eye with HORMS: 0.17 µm for a 4mm pupil (Figure 1.1A) and spot pattern that was used to generate the wavefront (Figure 1.1B). An example of a uncorrected highly aberrated eye with HORMS: 0.76 µm for a 4mm pupil (Figure 1.1C) and spot pattern that was used to generate the wavefront (Figure 1.1D).

The CCD camera in the wavefront sensor records an image of the spot field, and the intensity and location of each spot is analyzed with respect to a known reference location associated with a perfect optical system (no wavefront error). The X-Y displacement of each spot from its ideal location is used to calculate the tip and tilt (slope) of the wavefront at each local point in the pupil, and these local slopes are used to reconstruct the wavefront error over the pupil of the eye.

To quantify and communicate the amount of wavefront error present in an eye, the reconstructed wavefront error is fitted with the Zernike polynomial, which is the ANSI standard[8] for reporting aberrations of the eye. Fitting of the Zernike polynomial uses the least-squares method, and results in a series of coefficients, with each coefficient describing the amount of an individual aberration present in the wavefront error. Broadly speaking, the individual Zernike aberration terms are grouped together in a pyramidal shape based on the angular meridional frequency and radial order of the individual terms. These two components are used in the naming convention known as double index notation. For a double index notation, Zernike polynomials are arranged vertically by radial order (descending the pyramid equates to higher orders) and horizontally by angular frequency (moving out from the center of the pyramid equates to increased angular frequency). Zernike polynomials are also commonly defined by a single index notation, which starts at 0 increases from left to right, and top to bottom of the pyramid. Conversion from double to single index notation is possible using the following formula.

$$Zj = (n(n+2) + m)/2$$

Where j is the single index Zernike terms, n is the radial order and m is angular frequency.

Terms with a radial order ≤ 2 are known as lower-order aberrations and terms with a radial order > 2 are known as higher-order aberrations. Figure 1.2 pictorially represents the Zernike pyramid

with higher-order aberrations until the 5th radial order and labels the individual terms in both single and double index notation.

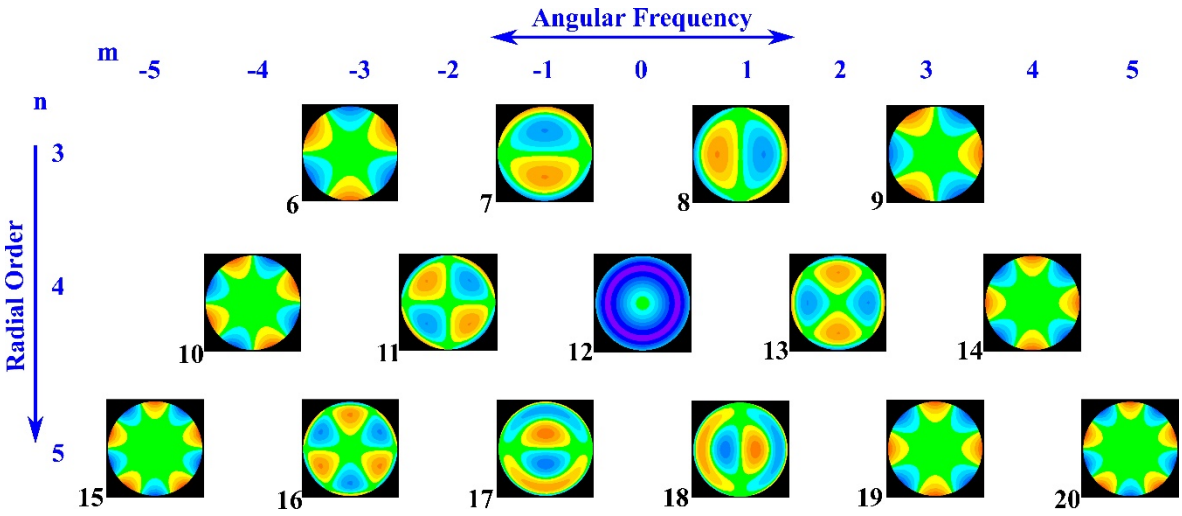

Figure 1.2 Zernike polynomials from 3rd to 5th radial order

While the Zernike polynomial provides an efficient method to characterize the individual aberrations that are present in the eye, there are other methods for communicating the impact of wavefront error. For instance, wavefront error can be further transformed into the point spread function (PSF),[9] which describes an image of a monochromatic point source of light in object space as it is imaged through the eye and onto the retina. The PSF is calculated as the squared modulus of the Fourier transform of the generalized pupil function, which is based on the wavefront error. If an eye were optically perfect (exhibiting no wavefront error) the PSF would be limited only by diffraction and would be recognizable as a point of light imaged onto the retinal. In reality, all eyes exhibit some level of wavefront error (both lower- and higher-order), which degrades the point spread function from the diffraction-limited case. Figure 1.3 shows a figure of a wavefront error, a PSF and a table of the Zernike coefficients that describe the wavefront that resulted in the measured PSF.

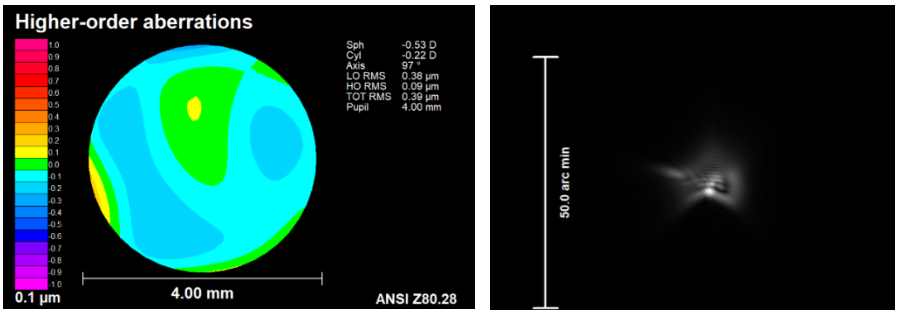

Terms	Radial order (n)	Frequency (m)	Coefficients (µm)
Single Index	Double Index		
0	0	0	0.000
1	1	-1	0.00
2	1	1	0.00
3	2	-2	0.023
4	2	0	0.370
5	2	2	0.088
6	3	-3	-0.011
7	3	-1	-0.047
8	3	1	-0.010
9	3	3	-0.031
10	4	-4	0.016
11	4	-2	0.014
12	4	0	0.038
13	4	2	0.028
14	4	4	-0.004
15	5	-5	-0.026
16	5	-3	0.019
17	5	-1	-0.007
18	5	1	-0.008
19	5	3	-0.006
20	5	5	0.001
21	6	-6	0.009
22	6	-4	-0.002
23	6	-2	-0.011
24	6	0	-0.006
25	6	2	-0.010
26	6	4	-0.005
27	6	6	-0.002

Figure 1.3 An example demonstrating higher-order root mean square map, point spread function and magnitude of each normalized Zernike coefficients. Root mean square is the calculated as the square root of sum of squares of each coefficients for a fixed pupil diameter.

1.4 Metrics based on measures of aberration (Diopters, RMS, PSF, Strehl, VSX)

Commonly, when describing the optical performance of the eye, a 10th order Zernike polynomial (or 66 individual Zernike aberration terms) is fitted to the measured wavefront error. The resulting coefficients are powerful in describing the individual optical errors present in the eye (e.g. defocus, coma, spherical aberration, trefoil, etc.), but this type of description is not useful in describing how the aggregate wavefront error as a whole impacts the resulting retinal image. To gain insight into how the optics of the eye as a whole influence retinal and visual image quality, researchers have developed single-value metrics (or metrics for short), which mathematically transform the Zernike coefficients that describe the wavefront error of the eye into a single value, where the value describes some aspect of the eye's optical or visual performance. The most commonly used metric is root mean square of the wavefront error (RMS).[9] This metric quantifies the magnitude of the difference of the eye's wavefront error from a plane wavefront, in terms of standard deviation. A common use of RMS wavefront error is to determine whether an eye is within or outside of an age-and-pupil-size-matched normative range for aberration terms in the higher orders (orders > 2). While commonly used, higher order RMS (or HORMS) is limited in that it does not consider the fact that different aberrations impact vision differently, and therefore the relationship between HORMS and visual performance is not monotonic.

The Strehl ratio[9] is a metric that is more common in pure optics than ophthalmic measurements, which compares the peak of the PSF of an eye (eye or refractive correction) with the diffraction limited PSF computed at the same pupil size. To better understand the visual consequence of wavefront error, the Strehl ratio has been evolved into visual image quality metric known as the visual Strehl ratio (VSX).[9,10] VSX is calculated by comparing the PSF of the eye with the

diffraction-limited PSF for the same pupil size, where both PSFs are weighted by the inverse Fourier transform of the neural contrast sensitivity function. It has been shown that VSX values worsen with age[10] and the effect becomes more pronounced in low luminance.[11] In addition, changes in VSX have been shown to predict changes in visual acuity.[12] VSX has also been used to objectively define optical corrections for the eye and to compare the effectiveness of different correction modalities.[13] In essence, VSX can act as a surrogate for visual performance. An instance where this might be advantageous would be when the number of correction conditions is impractical to test with actual patients, or when a "theoretical" correction is being evaluated before manufacture.[7]

1.5 Visual performance (acuity, contrast, reading)

Traditionally, distance high contrast visual acuity (VA) is the most commonly and universally accepted measure of visual function. VA utilizes a letter identification task to assess the ability of an eye to resolve increasingly higher spatial frequencies as the individual reads from the top to the bottom of the letter chart. While ubiquitous, high contrast acuity has been shown to be a relatively forgiving visual task, meaning that even in the presence of elevated levels of refractive error, individuals are able to perform reasonably well.[14] An ability to detect contrast has also been used as a measure of visual function. Contrast is defined as the difference in luminance between the visual target and the target background. [15] The reciprocal of the contrast threshold, which is defined as the minimum difference between the target and background that can be reliably detected, is the contrast sensitivity (CS). When CS is tested for a variety of targets of varying spatial frequency, a full CS function (or CSF) can be defined. Typically, the CSF exhibits the shape of a band pass filter, which consists of a low frequency roll-off, peak spatial frequency ~4 cycles/degree, and a high spatial frequency cut-off. With blur there is a decrease in

peak sensitivity and the high frequency cut-off shifts towards lower spatial frequencies. The generation of a full CSF for a subject can be cumbersome and time-consuming. An approximation of an individual's contrast sensitivity can be recorded using tests that employ letters of fixed angular size with decreasing contrast in addition to visual acuity testing. While VA and CS are both well-defined clinical tests, they do not necessarily reflect the full scope of the real-world challenges that face individuals in their daily lives. Tasks that begin to approximate these more real-world tasks include determining threshold word acuity (how small of a word is an individual able to read) and assessing reading speed (what duration is needed to accurately identify a word).

1.6 The relationship between aberrations and visual performance (in typical eyes and eyes with keratoconus)

It is a well-established fact that the elevated level of aberrations leads to reduction invisual performance. It has also been shown that reduced visual performance can lead to a measurable reduction in quality of life. Unfortunately, the way in which residual aberrations impact visual performance is complicated by the fact that individual aberrations do not equally affect visual performance.[16] Therefore, gaining a more complete understanding of the relationship between residual, uncorrected aberration and resulting visual performance on a host of visually relevant tasks is an important step in providing visual correction that will meet the individual needs of a patient in the clinic. This is particularly true in eyes that experience elevated levels of aberration, such as the aforementioned eyes suffering from the eye disease keratoconus.

While it is true that residual, uncorrected aberrations are present in all eyes (even the well-corrected, typically-sighted individuals) the impact of residual aberrations is amplified in keratoconus, where the vast majority of eyes exhibit elevated levels of higher-order aberration

even when wearing a conventional correction.[4–7] These residual uncorrected optical aberrations lead to reduced visual performance and visual image quality in individuals with keratoconus. From the patient's perspective, the visual percept in the presence of residual uncorrected aberrations can be complex, and often difficult to describe. Often patients with keratoconus comment on ghosting and doubling of images that persist even when wearing their conventional corrections.

Keratoconus serves as an ideal model to assess the impact of optical aberrations on visual performance, as these patients typically have good optical quality during the critical years of visual development, and only experience elevated aberrations after this critical period has ended. Keratoconus is a form of corneal ectasia where there is thinning of the corneal stroma that results in elevated higher-order aberrations. The prevalence rate of keratoconus has historically been reported as ~1/2000,[17] but more recent reports place the number at 1:375.[18] Though bilateral, there is a certain degree of asymmetry between the two eyes, which leads patients to commonly speak of their "good eye" and their "bad eye".

The collaborative longitudinal evaluation of keratoconus (CLEK)[19] study classifies keratoconus into three categories based on the steep keratometric power: mild (≤ 45 D), moderate (45 – 52 D) and severe (≥52 D). In the early stages of the disease, keratoconic eyes can be corrected with glasses, soft and small diameter rigid gas permeable contact lenses. As keratoconus progresses, the cornea tends towards a more conical shape, which induces higher-order aberration which render spectacles and soft contact lenses less effective at providing a satisfactory level of visual performance. Recently, the popularity of scleral lenses has increased significantly as a method for improving visual function and image quality in eyes with keratoconus. The index matching property of the fluid lens that is formed between the scleral lens and the anterior corneal surface

serves to reduce residual optical aberrations, leading to improved visual acuity, contrast sensitivity and visual image quality. However, a significant portion of eyes fit with scleral lenses still exhibit elevated levels of ocular aberration and poor visual image quality.[7] These residual aberrations, when present at significant amounts, can be targeted with individualized, customized scleral lenses (known as wavefront-guided lenses) that target the specific higher-order aberrations present in an individual eye. While they do provide superior visual performance, wavefront-guided corrections are very challenging to design and manufacture, and require a significant time and financial investment from both the practitioner and patient, and widespread adoption is limited due to the myriad challenges that face the practitioner when fitting the wavefront-guided lens. Importantly, the measured wavefront error of the eye must be placed over the pupil of the eye, meaning the optical correction is offset with respect to the geometric center of the lens. If simplification were possible, it is hypothesized adoption of wavefront-guided correction would increase, resulting in a larger segment of the keratoconus population meeting their visual needs, resulting in improved quality of life.

1.7 Gap in knowledge

This dissertation explores the manner in which typically-sighted individuals and individuals with keratoconus perform simulated, clinical and real-world visual tasks under varying levels uncorrected optical aberration. The work is divided into three experimental chapters (Chapters 2, 3 and 4) in this dissertation.

1.8 Brief overview of the experimental chapters

1.8.1 Chapter 2: The impact of misaligned wavefront-guided correction in a scleral lens for the highly aberrated eye

This study tested the viability of a common rather than individualized placement of the wavefront-guided aberration correction across a sample of highly aberrated eyes. The data set[6] consisted of 36 eyes of 18 individuals with keratoconus wearing their best corrected conventional scleral lens correction. Information about the residual aberrations and on-eye lens translations were used to simulate wavefront-guided corrections at both pupil and non-pupil centered locations.

1.8.2 Chapter 3: Word recognition thresholds as a function of disease severity in keratoconus

Previous study has shown that aberrations impact reading performance and the impact of individual aberrations on reading performance is unique to each aberration. As individuals with keratoconus have elevated aberrations originating from myriad individual Zernike modes, this study quantified visual performance in the presence of the combined aberrations on real world tasks (reading high and low contrast words with and without surrounding 4 flanking words). Nine individuals with keratoconus (18 habitually corrected eyes) and 6 typically-sighted individuals (12 habitually-corrected eyes) were recruited and participated in the study.

1.8.3 Chapter 4: Comparing the CamBlobs2 contrast sensitivity test to the near Pelli-Robson contrast sensitivity test in normally-sighted adults

This study sought to support expanding the clinical tests of visual function performed clinically by evaluating a novel test of contrast sensitivity, known as the CamBlobs2 test (Precision Vision, Woodstock, IL). In this experiment, the intra-visit repeatability and limits of agreement of the Camblobs2 test were compared to an existing test, the Pelli-Robson test (Precision Vision, Woodstock, IL). Twenty-two habitually corrected typically-sighted individuals participated in the study. In addition to these typical subjects, a small sample of 7 individuals with keratoconus was tested. These data are presented in Appendix of this dissertation.

Simply put: this dissertation seeks to gain insight into the impact of residual aberrations on resulting visual performance and does so with both typically-sighted individuals and individuals with keratoconus.

2 Chapter 2: The impact of misaligned wavefront-guided correction in a scleral lens for the highly aberrated eye

Reprinted with modifications from[7]: Rijal S, Hastings GD, Nguyen LC, Kauffman MJ, Applegate RA, Marsack JD. The impact of misaligned wavefront-guided correction in a scleral lens for the highly aberrated eye. Optom Vis Sci 2020;97;732-40.

2.1 Abstract

Significance: To achieve maximum visual benefit, wavefront-guided scleral lens corrections (WGCs) are aligned with the underlying wavefront error of each individual eye. This requirement adds complexity to the fitting process. With a view towards simplification in lens fitting, this study quantified the consequences of placing WGCs at two pre-defined locations.

Purpose: To quantify performance reduction accompanying placement of the WGC at two locations 1: the average decentered location (ADL - average decentration observed across individuals wearing scleral lenses) and 2: the geometric center (GC) of the lens.

Methods: De-identified residual aberration and lens translation data from 36 conventional scleral lens wearing eyes with corneal ectasia were used to simulate WGC correction *in silico*. The WGCs were decentered from the eye-specific pupil position to both the ADL and GC locations. The impact of these misalignments was assessed in terms of change (from the aligned, eye-specific pupil position) in higher order root mean square (HORMS) wavefront error, change in log of the visual strehl ratio (logVSX) and predicted change in logMAR visual acuity (VA).

Results: As expected, HORMS increased, logVSX decreased and predicted VA was poorer at both ADL and GC compared to the aligned condition ($P < .001$). Thirty four of 36 eyes had greater residual HORMS and 33 of 36 eyes had worse logVSX values at the GC than at the ADL. In clinical terms, 19 of 36 eyes at the ADL and 35 of 36 eyes at the GC had a predicted loss in VA of 3 letters or greater.

Conclusions: The placement of the WGC at either ADL or GC is predicted to lead to a noticeable reduction in VA for over half of the eyes studied, suggesting the simplification of the fitting process is not worth the cost in performance.

2.2 Introduction

Wavefront-guided scleral lenses are designed to reduce the elevated residual aberrations that continue to exist during conventional scleral lens wear in patients with corneal ectasia,[4–6,20–22] and have been shown to provide superior visual acuity, contrast sensitivity[1,2] and visual image quality[6] when compared to conventional scleral lenses. Unlike the design of spherical or sphero-cylindrical scleral lenses, the design of wavefront-guided scleral lenses requires information regarding the residual lower and higher-order aberrations measured through a well-fitted conventional scleral lens, as well as information concerning the on-eye decentration of the lens with respect to the eye's pupil.[4–6] These latter data are necessary due to the fact that for the wavefront-guided correction to perform ideally, the wavefront-guided correction must be registered with the underlying wavefront error. Since scleral lenses typically settle inferior and temporal with respect to the pupil center,[6,23–28] the wavefront-guided correction is typically displaced superiorly and nasally from the geometric center of the lens to align with the pupil. However, this requirement to individually position the wavefront-guided optics in an eye - specific manner adds another level of personalization and complexity to the wavefront-guided fitting process. And since quantification of these misalignment data are not a part of common clinical practice, their measurement forms yet another technical and intellectual barrier to the delivery of wavefront-guided corrections.

There is a history of conceding that the absolute highest theoretical level of optical and visual performance is not achievable with a wavefront-guided scleral lens, given the real-world clinical constraints associated with alignment uncertainties. Previous studies[29,30] have attempted to partially correct higher-order Zernike aberration terms to optimize wavefront-guided corrections in the presence of registration uncertainty. A portion of this prior work was built on

the observation that scleral lenses naturally move (to some degree) on the eye, and ideal performance at all times is simply not possible.[30] Therefore, the goal was to optimize performance *in the presence of observed translations and rotations*, knowing that some decrease in performance from the ideally aligned condition would be observed at all misaligned locations.

In the current study, another compromise is examined: that is, if placement of the wavefront-guided correction was not considered on an individual basis, but was applied in a consistent manner to all individuals in a population. The question being asked here was not whether this misalignment would lead to a reduction in performance (it will),[31–33] but instead whether the loss would be acceptable in terms of high contrast visual acuity, given the simplification that the potential use of these locations would afford the clinician attempting to fit the wavefront-guided correction. The two locations studied here were:

1. The average decentered location defined as the mean horizontal and vertical translation of the conventional scleral lenses.
2. The geometric center of each scleral lens.

These two locations were studied relative to the eye-specific pupil center.

This study highlights the challenges associated with wavefront-guided corrections. It clearly demonstrates that these corrections are highly individual in nature and emphasizes that the success of wavefront-guided corrections finds its foundation in the myriad details being correct (in this case, alignment of the correction with respect to the measured wavefront error).

2.3 Methods

2.3.1 Aberration data

De-identified data representing 21 individuals (mean age: 40.3 ± 10.2 years) diagnosed with corneal ectasia were obtained from a prior study[6] on the performance of wavefront-guided scleral lenses. These data include the residual, uncorrected 2nd-10th order Zernike aberrations measured during conventional scleral lens wear, as well as decentration data. Zernike coefficients with odd symmetry along the vertical axis in left eyes were multiplied by -1.00, such that all eyes studied represented "right eyes".[8]

The dilated residual aberrations through conventional scleral lenses were rescaled to a 5mm pupil diameter[34] and the higher-order root mean square wavefront error through the 6th radial order was calculated[9] for 36 eyes (18 individuals) with corneal ectasia as shown in Figure 2.1. Three of the original 21 individual's data were excluded, and this exclusion is described in detail below. Conventional scleral lenses provide a new smooth refractive surface over the irregular cornea and allows approximate matching of the refractive index of the cornea with that of the tears, which reduces the aberrations of the ectatic eyes. This masking of aberrations moves some eyes into the normal range of total higher-order aberrations.[2,6] Twelve of the 36 eyes (white bars in Figure 2.1) studied here were within mean ± 2 standard deviation of higher-order root mean square wavefront error for typical eyes for a 5mm pupil diameter (less than 0.342μm).[2] That said, aberrations are known to interact visually, and these interactions alter visual image quality.[16,35,36] Visual image quality measured in terms of log of the visual Strehl ratio was reduced in 31 out of 36 eyes compared to the normative population (mean ± 2SD, -0.493 ± 0.304)[10] for a 5mm pupil diameter.

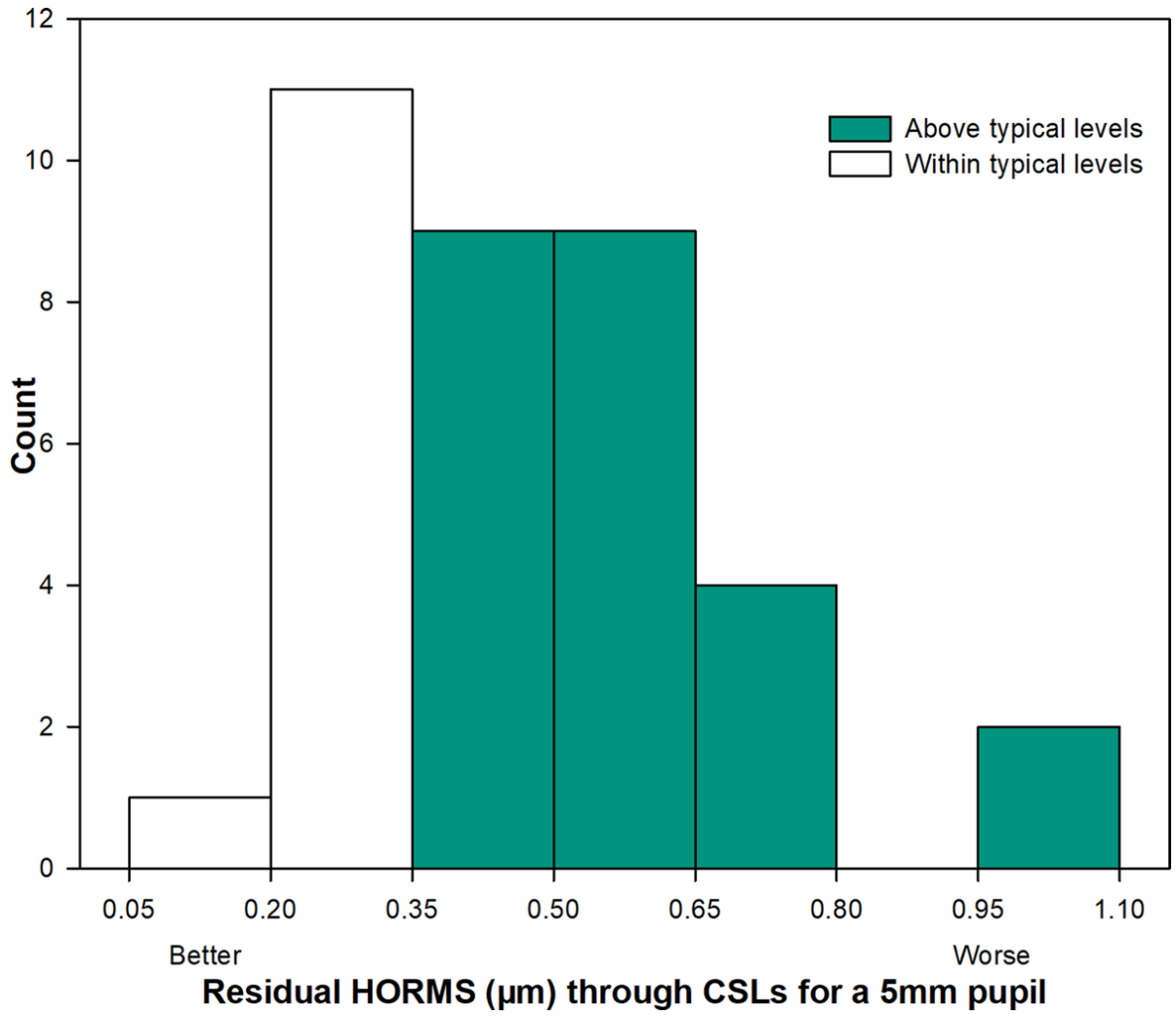

Figure 2.1 Residual higher-order root mean square wavefront error (HORMS; in micrometers) over a 5-mm pupil through the sixth radial order observed in 36 eyes with corneal ectasia, measured through best conventional scleral lenses (CSLs). White bars represent eyes within mean ± 2 standard deviations (SD) of typical eyes for a 5-mm pupil diameter, and green bars represent eyes above the mean + 2 SD levels for HORMS. Residual aberrations were elevated in 67% of the eyes compared with normative levels (mean + 2 SD of typical individuals being less than 0.342 µm).[2]

2.3.2 Scleral lens and pupil decentration data

The amount of decentration for each conventional scleral lens was defined as the Cartesian (x, y) distances of the pupil center relative to the geometric center of the lens (Figure 2.2). These decentration data were obtained by first recording a series of images of the conventional scleral lens on the eye. As with aberration data, values for the x component of the decentration in left eyes were multiplied by -1.00 to represent right eyes. The average decentered location (mm) across all eyes in the horizontal and vertical meridians was calculated as x: 0.53 (temporal) and y: 0.56 (inferior), which are traditionally compensated by a nasal and superior shift of the wavefront-guided correction relative to the geometric lens center when designing the wavefront-guided lens. For modeling purposes, it is assumed that the optical axis of all measurement instruments were aligned to the line of sight (the line connecting the fixation point and the center of the eye's entrance pupil) with the patient fixation target being co-axial with the instrument axis and located slightly beyond optical infinity, and that the eyes optical aberrations and optical correction existed in the same plane. The vector length was defined as the square root of the sum of the squares of the horizontal and vertical lens decentration from the eye-specific pupil center.

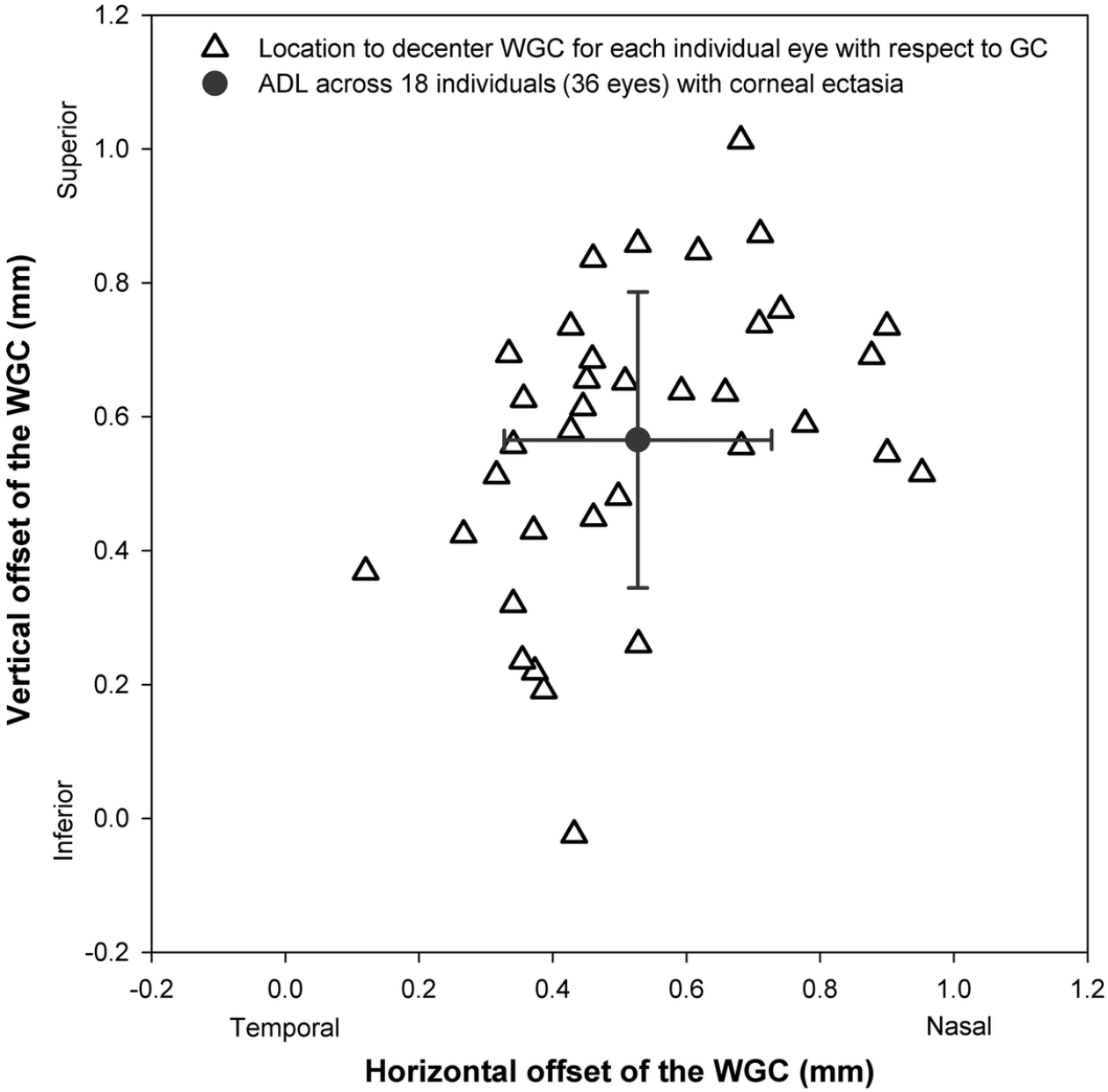

Figure 2.2 The magnitude of translation required to offset the wavefront-guided correction (WGC) from the geometric center (GC) (0, 0) to the pupil center (from the origin to each open triangle) and to the average decentered location (ADL) (from each triangle to the gray solid circle) across 36 eyes of individuals with corneal ectasia. These data illustrate the clinical observation that a typical WGC is shifted superior-nasal from the geometric center to compensate for inferotemporal displacement of the conventional scleral lens.

2.3.3 Simulation of wavefront-guided correction and quantification of change in optical and visual performance at the two common locations

All measured residual aberration data included in this study were defined over a pupil diameter greater than 6.5 mm. Consequently the data of 3 individuals were excluded from the current study due to the fact that their dilated pupil diameter was less than 6.5 mm and thus, would not satisfy the condition that the translated wavefront-guided correction needed to overlap the final pupil diameter of interest (5mm) entirely. Wavefront-guided lenses incorporating the wavefront-guided corrections at the average decentered location and geometric center were not physically constructed. Rather, the corrections were computationally simulated, starting with the multiplication of all residual aberration coefficients measured during conventional scleral lens wear by -1.00, resulting in an ideal wavefront-guided correction for each individual eye through the 10th radial order. The correction that was applied during simulation to the residual aberration measured on the eye only included 2nd to 5th radial order terms (setting 6th to 10th radial order terms of the correction to zero). The decision on which orders to include in the correction was based on a desire to mirror the implementation of actual corrections in prior work.[2,3] The portion of the wavefront-guided correction following translation from the eye-specific pupil position (pupil center) to the position of interest (either the average decentered location or the geometric center of the lens) was calculated. The previously published MATLAB (Math works, Inc. USA), methods described by Dr. George Dai[34] were reproduced by the investigators and employed for all misalignments and resizing of aberrations. Prior to use in this study, the MATLAB implementation was validated through replication of results presented by Dai.[34] Aberrations through the 10th Zernike radial orders at the pupil center, average decentered location, and geometric center were resized to the pupil diameter of 5mm. The wavefront error defining the

correction over the eye-specific pupil position (pupil center), average decentered location, or the geometric center were added to the residual aberrations measured through the best conventional scleral lens to simulate optical performance of the wavefront-guided scleral lens at each of the three locations.

The change in vertical and horizontal coma was calculated at the average decentered locations and geometric center from pupil center from the simulated residual aberrations through wavefront-guided scleral lens. The change in higher-order root mean square wavefront error was also calculated for average decentered location and geometric center from the pupil center. The eye with vector length closest to the median measured from the eye-specific pupil center to the geometric center is shown in Figure 2.3.While the increase in higher-order root mean square wavefront-error was anticipated, it cannot unambiguously be used to assess the potential visual impact associated with placing the wavefront-guided correction at the average decentered location or geometric center because it does not consider the interactions of aberrations[10,16,36] and their impact on visual performance.[37] In order to better quantify the visual consequence of placing the wavefront-guided correction at the eye-specific pupil location, average decentered location or the geometric center, logVSX[9] was calculated from residual 2nd -10th order aberrations. For reference, a logVSX value of 0 represents the best possible visual image quality. As the value decreases (becomes more negative), logVSX represents a worsening level of visual image quality.

2.3.4 Predicting change in LogMAR visual acuity from the change in log of the visual strehl ratio (Logvsx)

The change in logVSX at the average decentered location and the geometric center of each lens with respect to the eye-specific pupil center were calculated. The changes in logVSX were, in turn, used to predict change in logMAR visual acuity using the following equation:

$$\text{Change in logMAR visual acuity} = -0.2558 * \text{change in logVSX.} \quad (1)$$

This equation is an evolved version of a previous published equation[12] defining change in logMAR visual acuity as a function of change in logVSX, which is defined such that even when there was no change in logVSX, there is a predicted change in logMAR visual acuity of 1.5 letters.[12] To address this, the data from the previous study were refit, and the modified equation (Equation 1) was used here.

Statistical analyses

Mann-Whitney rank sum test was used to compare the vector length between average decentered location and geometric center. Repeated measures analysis of variance on ranks with post-hoc Tukey test was used for comparison between average decentered and geometric center locations, as compared to the pupil center. Correlation analysis was used to determine the relationship between vector length and predicted change in acuity at both average decentered location and geometric center.

2.4 Results

Figure 2.3 reports an example of 3rd-10th order higher-order aberrations over a 5mm pupil for a representative eye (vector length is closest to the median) when the correction is a) well-centered at eye-specific pupil center, b) decentered to the average decentered location and c) decentered to the geometric center. In Figures 2.4-2.7 below, gray transparent bars represent changes observed when the correction is applied at the average decentered location and green bars represent changes observed when the correction is applied at the geometric center. Figures 2.4-2.7 contain a red 'x', denoting the eye represented in Figure 2.3. For each graph, the change from the eye-specific pupil center to the average decentered location or the geometric center for the same eye is plotted together for comparison. The order of eyes presented in Figures 2.5-2.7 is consistent with the ordering of eyes used in Figure 2.4.

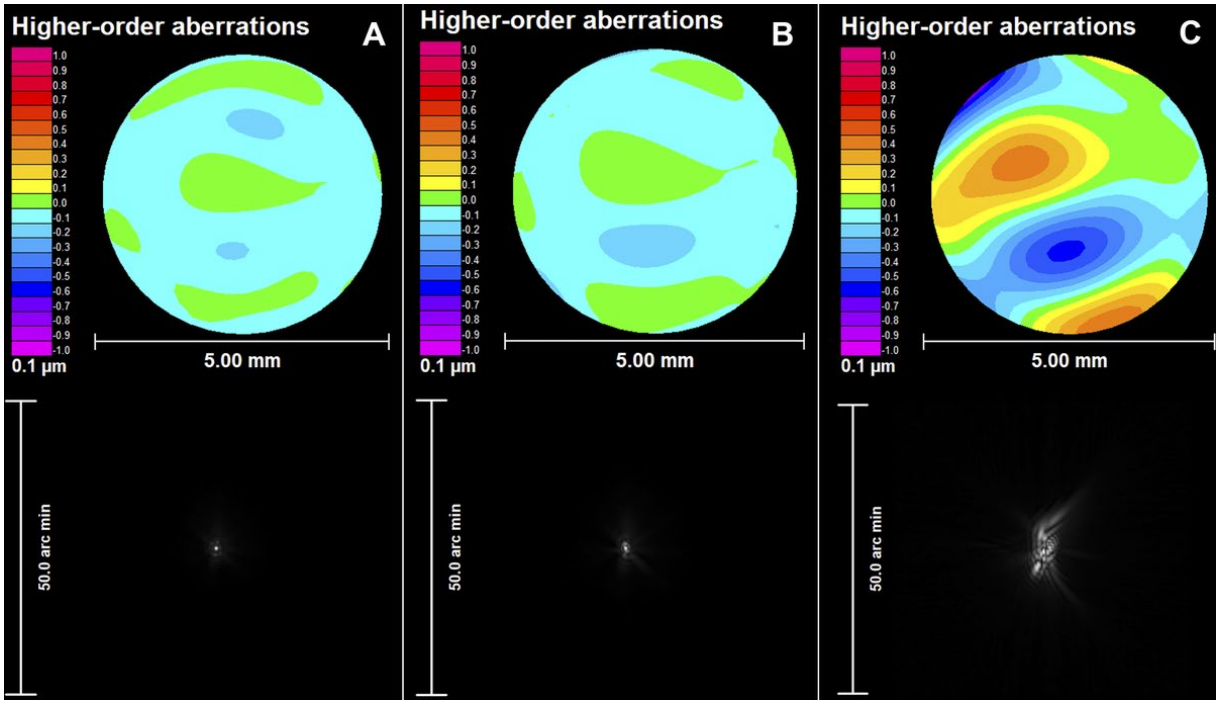

Figure 2.3 An example representing residual higher-order wavefront error and point spread functions from the (A) eye-specific pupil center (HORMS: 0.04 µm), (B) average decentered location (vector length, 0.14 mm; HORMS, 0.05 µm), and (C) geometric center (vector length, 0.82 mm; HORMS, 0.24 µm) for one eye.

2.4.1 Vector length from the pupil to the average decentered location and the geometric center

The average ± standard deviation vector length (mm) to translate from the eye-specific pupil center to the average decentered location was 0.27 ± 0.13 (first quartile (1Q): 0.15, median (M): 0.27, third quartile (3Q): 0.37) and to the geometric center was 0.79 ± 0. 24 (first quartile (1Q): 0.60, median (M): 0.81, third quartile (3Q): 1.02). Thirty four out of 36 eyes (Figure 2.4) at the average decentered location had shorter vector length compared to the geometric center ($P <$ 0.001)

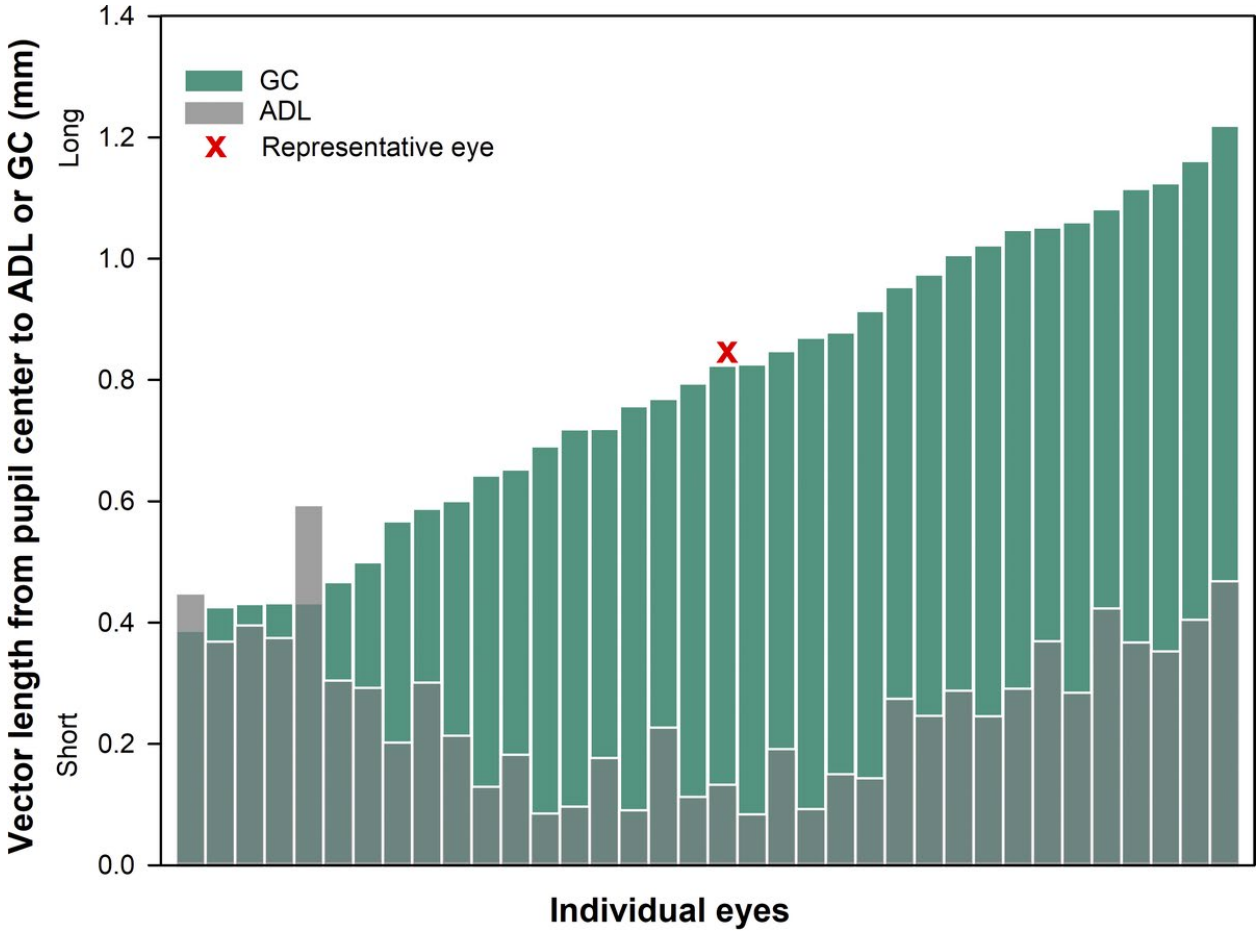

Figure 2.4 Vector length (in millimeters) from the eye-specific pupil center to the average decentered location (ADL; gray translucent bars) and geometric center (GC; green bars) for each individual eye. The location of the geometric center was farther than the average decentered location for 34 of 36 eyes.

2.4.2 Change in coma and higher-order root mean square wavefront error

The average ± standard deviation change in vertical coma (μm) at the average decentered location was 0.026 ± 0.070 (first quartile (1Q): -0.018, median (M): 0.020, third quartile (3Q): 0.059). At the geometric center, the values were 0.202 ± 0.231 (first quartile (1Q):0.035, median (M): 0.194, third quartile (3Q): 0.393) at the geometric center. The average ± standard deviation change in horizontal coma (μm) at average decentered location was -0.012 ± 0.056 (first quartile (1Q):-0.035, median (M): -0.005, third quartile (3Q): 0.018) and 0.033 ± 0.158 (first quartile (1Q): -0.067, median (M):0.016, third quartile (3Q): 0.123) at the geometric center. The average ± standard deviation change in higher-order root mean square wavefront error (μm) when the wavefront-compensating optics were moved to the average decentered location was 0.09 ± 0.06 (first quartile (1Q): 0.04, median (M): 0.08, third quartile (3Q): 0.13) and the average ± standard deviation change in higher-order root mean square wavefront error (μm) when the wavefront-compensating optics were moved to the geometric center was 0.38 ± 0. 21 (first quartile (1Q): 0.18, median (M): (0.41, third quartile (3Q): 0.54). Thirty four out of 36 eyes (Figures 2.4 and 2.5) at the geometric center had greater change in higher-order root mean square wavefront error compared to the average decentered location. As expected, there was a statistically significant difference in higher-order root mean square wavefront error when the wavefront-guided correction was misaligned to the either average decentered location or the geometric center of the lens rather than to the eye-specific pupil position (both $P < .001$).

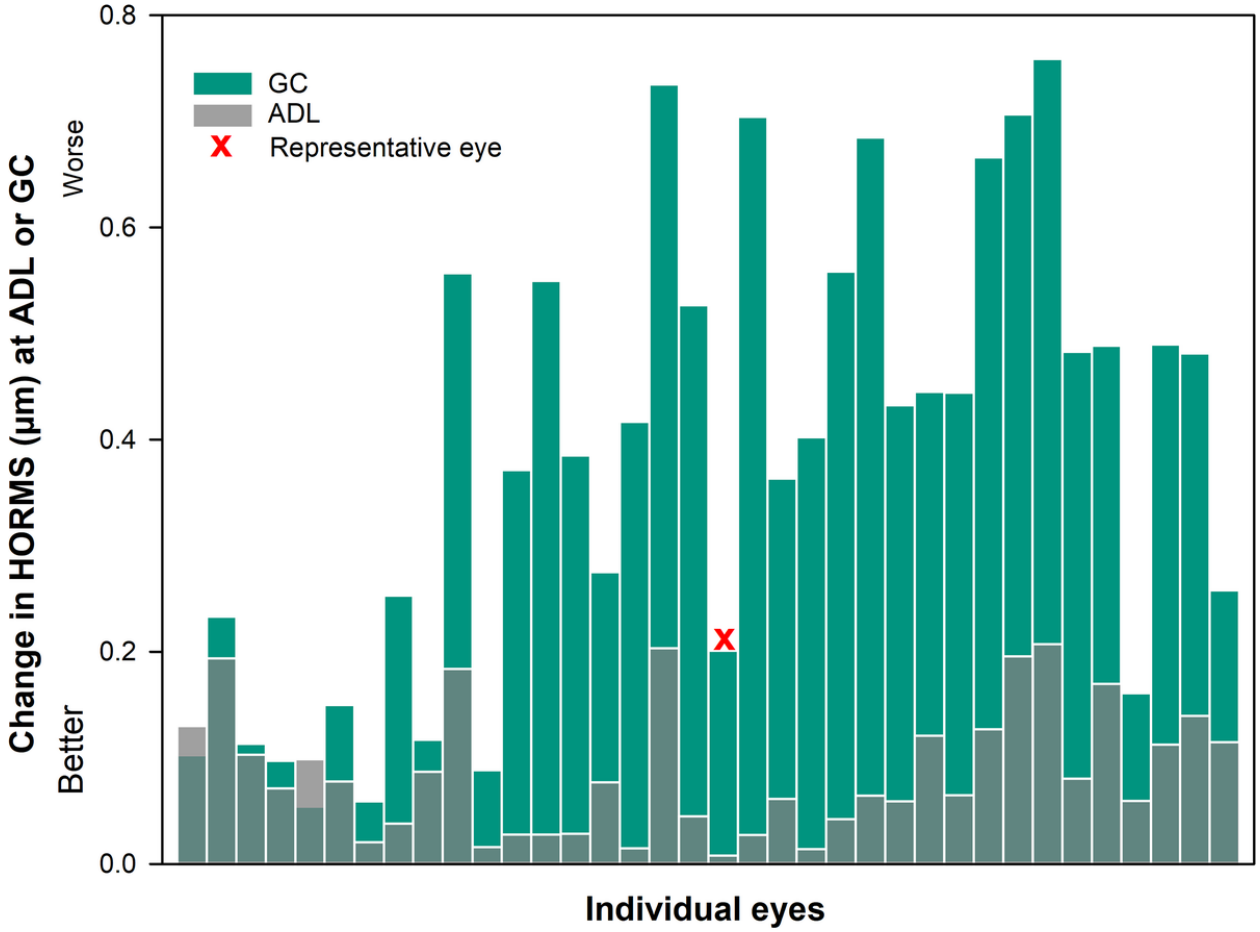

Figure 2.5 The change in higher-order root mean square (HORMS) wavefront error (in micrometers) over a 5-mm pupil from the eye-specific pupil center to the average decentered location (ADL; gray translucent bars) and geometric center (GC; green bars) for each individual eye. The change in HORMS (in micrometers) was greater at the geometric center than at the average decentered location for 34 of 36 eyes.

2.4.3 Change in log of the visual strehl ratio (LogVSX)

Average ± standard deviation change in logVSX observed at the average decentered location was -0.31 ± 0.20 (first quartile (1Q): -0.50, median (M): -0.27, third quartile (3Q): -0.14) and the average ± standard deviation change in logVSX for geometric center was -0.92 ± 0.45 (first quartile (1Q): -1.23, median (M): -0.86, third quartile (3Q): -0.64). Thirty three out of 36 eyes (figure 2.6) had greater change in logVSX at the geometric center compared to the average decentered location .There was a statistically significant difference in the change in logVSX when the wavefront-guided correction was misaligned to either average decentered location or the geometric center of the lens, rather than to the eye-specific pupil position (pupil center) (both $P < .001$).

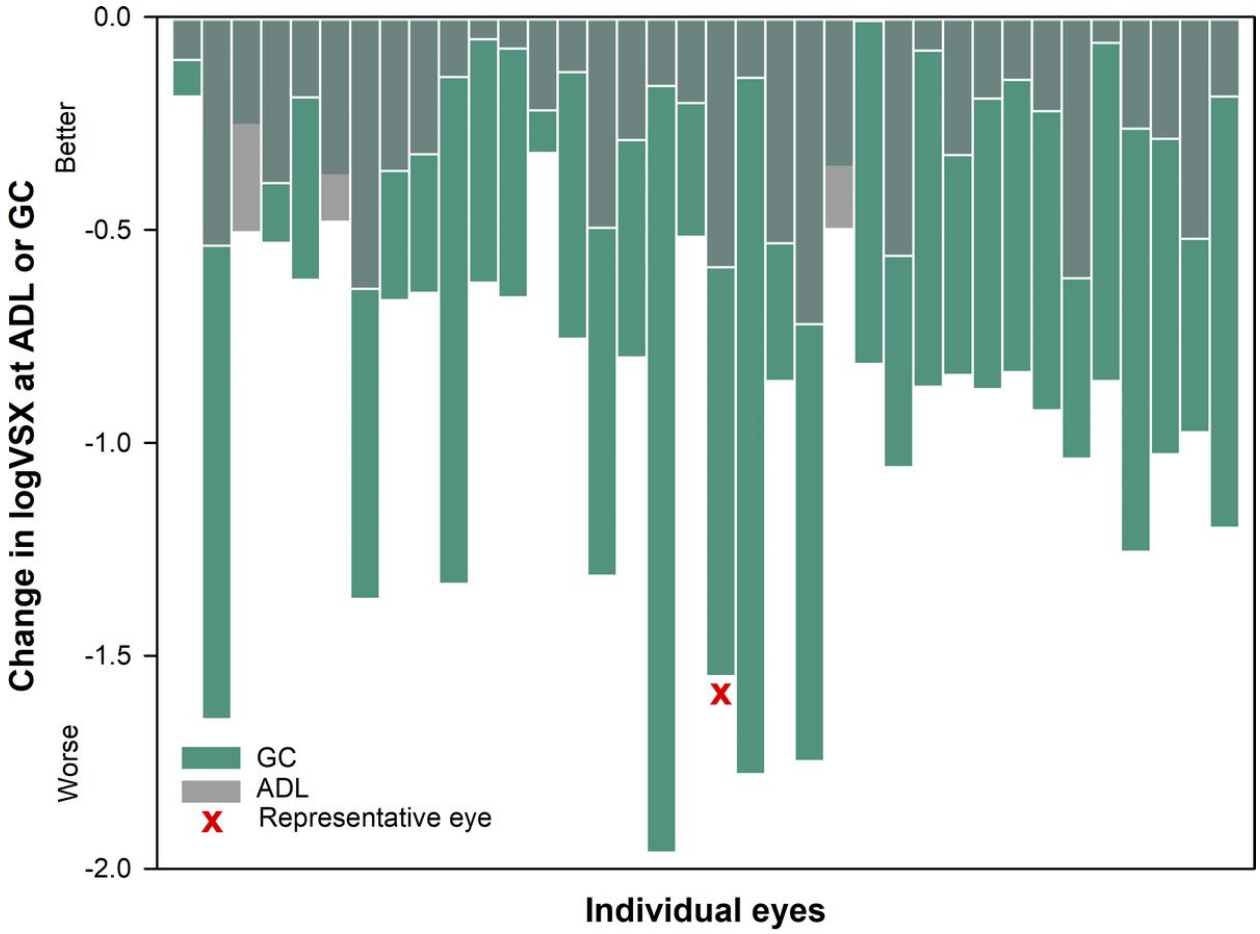

Figure 2.6 The change in log of the visual Strehl ratio (logVSX) over a 5-mm pupil from the eye-specific pupil center to the average decentered location (ADL; gray translucent bars) and geometric center (GC; green bars) for each individual eye. The change in logVSX was smaller at the average decentered location than the geometric center for 33 of 36 eyes.

2.4.4 Calculating predicted change in LogMAR visual acuity based on change in LogVSX

The average ± standard deviation change in predicted logMAR visual acuity at the average decentered location was 0.08 ± 0.05 (first quartile (1Q): 0.04, median (M): 0.07, third quartile (3Q): 0.13) and the average ± standard deviation change in logMAR visual acuity for geometric center was 0.24 ± 0.11 (first quartile (1Q): 0.16, median (M): 0.22, third quartile (3Q): 0.31).All measurements are made relative to the eye-specific pupil center. Thirty three out of 36 eyes (Figure 2.7) had greater predicted change in logMAR visual acuity at the geometric center compared to the average decentered location. There was a statistically significant difference in change in logMAR visual acuity when the wavefront-guided correction was misaligned to either average decentered location or the geometric center of the lens rather than to the eye-specific pupil center (both $P < .001$). From a clinical perspective, 19 out of 36 eyes at the average decentered location and 35 out of 36 eyes at the geometric center of the lens had a loss in predicted logMAR visual acuity by more than 3 letters, which is a reported level of test-retest reliability of visual acuity measurements.[13,38,39]

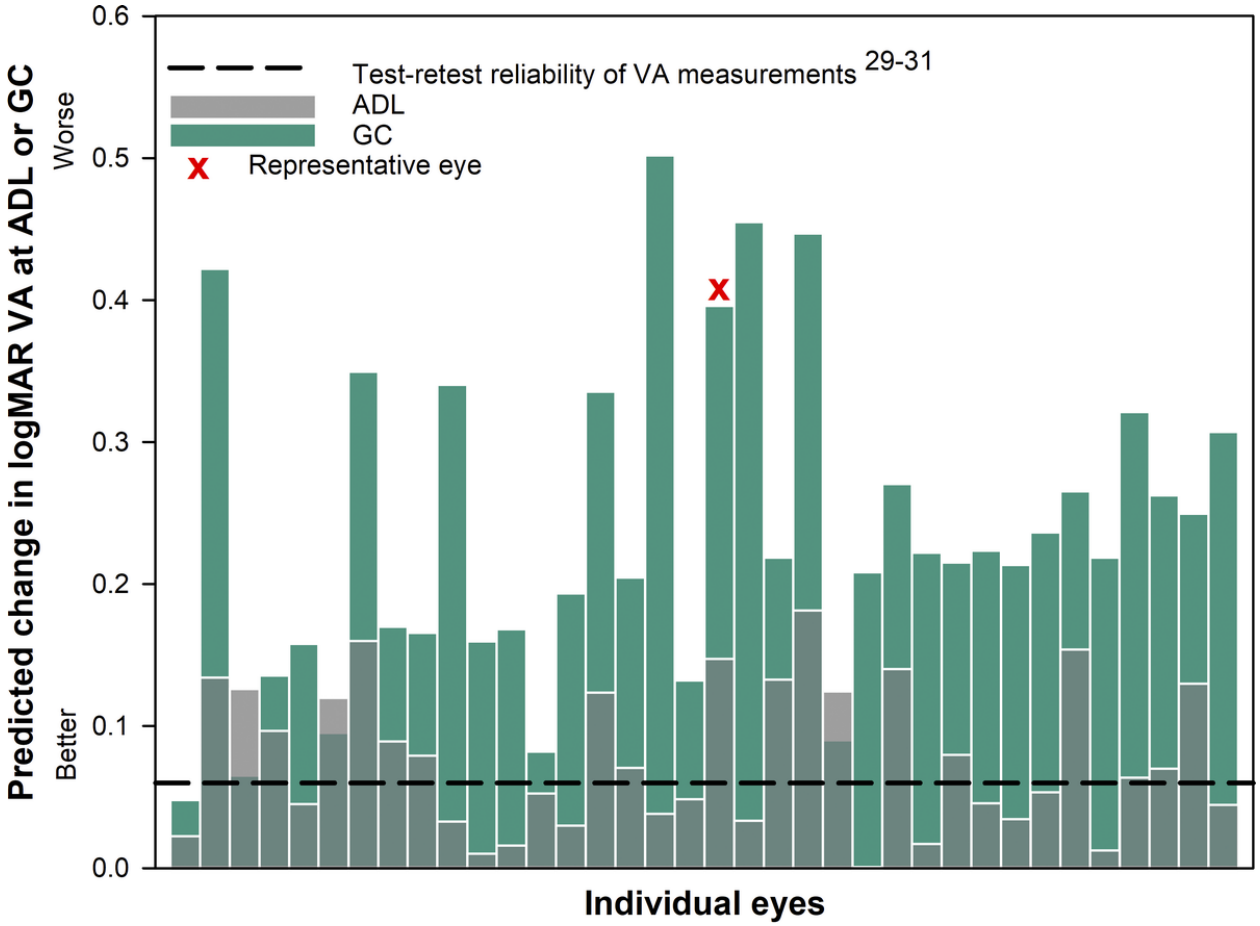

Figure 2.7 The predicted loss in logMAR visual acuity[12] for each individual eye with corneal ectasia when the wavefront-guided correction was located at the average decentered location (ADL; gray translucent bars) and the geometric center (GC; green bars) of each scleral lens. The dashed black line represents the threshold change of 0.06 logMAR or three letters based on test-retest reliability of acuity measurements.[13,38,39] Nineteen of 36 eyes at the ADL and 35 of 36 eyes at the GC had a predicted loss in visual acuity of more than three letters (0.06 logMAR).

2.5 Discussion

The goal of this study was not to quantify whether placing a wavefront-guided correction at two non-pupil centered locations (the average decentered location and the geometric center of each lens) would lead to a loss in optical and visual performance, it was known that such offsets would lead to such losses.[29,31,40] Instead, the goal was to test the viability of a common, rather than individualized, decentration rule across eyes. The results suggest that the change in higher-order root mean square wavefront error, visual image quality, and predicted change in logMAR visual acuity were significant at both locations when compared to the eye-specific pupil center. Importantly, the average change in logMAR visual acuity anticipated at either location exceeded the test-retest reliability for high contrast logMAR visual acuity of 3 letters for more than half of eyes studied.[13,38,39]

In this study, the actual translation and underlying residual aberrations through conventional scleral lenses were used, and the eyes with the greatest level of decentration do not necessarily have the greatest change in higher-order root mean square, logVSX or predicted change in visual acuity. The correlation (R^2) between vector length and predicted change in acuity was 0.00 at the average decentered location and 0.07 at the geometric center, highlighting the fact that the interactions between individual terms,[16,35,36] and not simply vector length, are important factors in understanding visual impact. This is expected, as the magnitudes and direction of translation in both horizontal and vertical meridians, as well as eye-specific levels of residual uncorrected aberration all play a complex, interconnecting role in the resultant impact on an individual's performance. Shi et al.[30] suggested that the translation and rotation of the lens induce asymmetrical optical tolerance to movement and induced errors are depended on the underlying wavefront error, the wavefront-guided correction design, and the amount of

registration error. Shi et al.[30] also reported that the registration tolerance to maintain good visual acuity is unique for each wavefront error and wavefront-guided correction design. These questions were not addressed on an individual level in the current work, rather the question that was addressed was more direct: can one of these two locations be used universally in this population? Considering the answer to this question on the basis of a group was necessary, if either location were to be adopted for use clinically on any and all individuals with ectatic corneas seeking wavefront-guided correction. The answer was that the use of either location left a significant portion of eyes with visual deficit from the eye-specific pupil center.

Given the fact that wavefront-guided lenses are so highly customized, such a compromise would only be accepted if the consequence of that compromise was small. We chose a strict criterion of logMAR visual acuity loss of 3 letters (0.06 logMAR) for identifying a meaningful change in visual acuity at the average decentered and geometric center locations. Use of either the average decentered location or the geometric center as a common location for placement of the correction led to a predicted change in visual acuity that, exceeded this 3 letter benchmark for over half of the eyes studied. This work was intended to provide insight to the clinical community that for custom wavefront-guided scleral corrections, the optics must be aligned to the underlying wavefront error measured over the pupil.

This study has several limitations. The results presented here are derived from simulation and do not consider the dynamic movement of the lens on-eye (small levels of dynamic lens translation and rotation) which may occur with blink. The effect of the tear film and tear break up time is also not considered in this simulation while calculating final residual aberrations through the wavefront-guided correction. Also, scleral lenses are a specialty device and wavefront-guided scleral lenses make up a small portion of the scleral lens management.

However, scleral lenses are gaining popularity with their broader applications for other ocular surface conditions.[23] Wavefront-guided scleral lens corrections are the unrivaled options for some highly-aberrated eyes and have helped with the recent resurgence of scleral lenses. [6,41] Conceptually demonstrative papers like this are necessary to increase the use and adoption of these technologies.

In conclusion, decentering the wavefront-guided correction to either the average decentered location or the geometric center leads to elevated residual higher-order aberrations and reduced visual image quality at levels that are predicted to reduce visual acuity on average by more than three letters in the majority of cases. This level of deficit is expected to be noticeable to the patient, suggesting the simplification that would be gained in the fitting process is not worth the cost in terms of visual and optical performance.

Acknowledgments

Dr. Ayeswarya Ravikumar for assistance with the predictive model. Dr. Larry Thibos and Hope Queener for the metrics calculation. Dr. Ed and Charlene Sarver of Sarver and Associates for use of Visual Optics Laboratory.

3 Chapter 3: Quantification of near word acuity thresholds with and without flankers for individuals with keratoconus

3.1 Abstract

Purpose: Residual lower- and higher-order aberrations can be elevated in the eyes of individuals with keratoconus, even in the presence of habitually prescribed refractive corrections. The purpose of this study was to quantify visual performance in the presence of these residual aberrations on real world tasks involving word recognition

Methods: Nine individuals with keratoconus and six typically-sighted individuals were included in the study. LogMAR 100% high contrast (HC) and 25% low contrast (LC) near visual acuity (NVA) were recorded at 40 cm. Residual aberrations while wearing habitual correction were measured with a COAS-HD wavefront sensor and analyzed over a 4mm pupil. Corneal topography was quantified with a Pentacam corneal topographer and used to quantify disease severity. Subjects were asked to read aloud single words monocularly (with and without flanking words) for HC and LC conditions at 40cm. The words were presented at 5 font sizes (up to 3 lines above HCNVA and 4 lines above LCNVA) in Arial font and presented at 5 stimulus durations (50, 125,250, 500, 1000 miliseconds) for a total of 1000 word reading trials/eye. Psychometric functions were fitted, and thresholds were defined as 80% correct for each font size and duration.

Results: As defined by the CLEK study, five eyes had mild, 9 eyes had moderate and 4 eye had severe keratoconus. The mean difference in distance visual acuity, high contrast near visual acuity, low contrast near visual acuity between the worse and the better eyes were 0.18 ± 0.18, 0.19 ± 0.20, 0.25 ± 0.26 in the keratoconus group and 0.06 ± 0.03, 0.08 ± 0.13, 0.01 ± 0.08 in the typically-sighted group. Eyes with keratoconus had greater threshold logMAR acuity and variability than typically-sighted individuals for all stimulus durations. There was a trend for elevated threshold word acuity compared to visual acuity, more pronounced with low contrast

words. Threshold word acuity for the better eye were better than for the worse eye for individuals with keratoconus.

Conclusions: Word recognition thresholds were elevated compared to distance high contrast visual acuity. There existed asymmetry in word recognition thresholds between the better and the worse eye in individuals with keratoconus.

3.2 Introduction

High contrast visual acuity is the gold standard for visual function testing.[42–44] This easy to record clinical measure also has the advantage of a significant normative database available in the literature,[13,38,39] making it easy to compare the visual acuity of an individual in the clinic or laboratory setting to that of a "typical" individual. Despite its ubiquity, high contrast visual acuity does have limitations. First, it is a quantitative measure of visual performance, meaning it does not necessarily reflect the patient's satisfaction with their visual quality. This is seen acutely in the 20/20 unhappy patient who may report "I can read the letters, but they are not clear."[14] Being insensitive to the quality of the visual percept,[14] it may overestimate performance on more complex tasks, such as word recognition and reading. The process of reading represents an increase in task complexity from the simple letter identification task found in high contrast visual acuity, and involves deconstructing the visual input originating from text and encoding it into meaningful concepts.[45–47] Further, the task of reading occurs under a much wider variety of conditions (eg.: contrast, duration) than high contrast visual acuity.

The process of reading can be disrupted by external factors, such as typographical errors, or internal factors resulting from ocular[48–50] and neurological disease,[51,52] reducing reading performance. One disease that affects the optical, and therefore, image-forming capabilities of the visual system is keratoconus.[1] Keratoconus is a progressive bilateral eye disease with an estimated prevalence rate as high as 1:375.[17,18] Even with the current advanced optical correction methods , individuals with keratoconus have elevated levels of both lower- and higher-order aberrations.[4–7]

As in typical eyes, high contrast visual acuity is used clinically to assess the visual consequence of keratoconus, but as this task is one of simple identification, it may fail to report the reduced

visual quality and more contextualized real-world function that occurs when letters are strung together to make words, where words are used to form sentences, and where the presentation of the stimulus can be modulated in both time and contrast. Evidence for these deleterious effects can be found in quality of life surveys, which demonstrated that reading ability was reduced with the progression of keratoconus, resulting in a reduction in quality of life.[53,54] While reading is an extremely important task, little is known regarding the mechanisms by which keratoconus impacts word recognition and reading. Systematic simulation studies have assessed reading performance using individual lower- and higher order aberration terms.[49,50,55] However, aberrations interact with each other and individual aberrations do not affect vision equally.[16,35,36] Neural factors, such as adaptation, also play a role in interpretation for the visual percept.[56,57] These early studies demonstrate the challenges associated with developing laboratory-based tests that accurately reflect real-world demands associated with daily living, such word recognition as reading.

As a step toward understanding the impact keratoconus has on reading ability, the aim of this study was to quantify threshold word acuity with and without flanking words for different stimulus durations, and contrasts at near (40cm) in individuals with keratoconus and typically-sighted individuals wearing their habitual corrections.

3.2 Methods

All procedures adhered to the tenets of the Declaration of Helsinki. All subjects signed an informed consent document prior to the administration of any testing. Experimental protocols were approved by the Institutional Review Board at the University of Houston.

3.2.1 Subjects

Nine individuals with clinically diagnosed keratoconus and 6 typically-sighted subjects were included in this study. Subjects completed all testing while wearing their habitual correction (spectacles and contact lenses, if any). All typically-sighted individuals had habitual visual acuity of 20/25 or better, while individuals with keratoconus were recruited with the goal of enrolling a broad spectrum of disease severity (mild to severe, as classified by the Collaborative Longitudinal Evaluation of Keratoconus study group).[19] With this as the goal, any level of acuity was accepted in the keratoconus sample.

3.2.2 Accommodation

As word recognition ability was tested at 40cm, subjective accommodative amplitude was first assessed with the push-up technique to ensure subjects had an accommodative amplitude > +2.50D to overcome the near stimulus demand (+ 2.50D at 40cm).

3.2.3 Visual acuity

High (100%) and low (25%) contrast logMAR visual acuity was recorded monocularly at two distances: 4m (distant) and 40cm (near). LogMAR acuity charts (Good-Lite, Elgin, IL) were used and a letter-by-letter scoring paradigm was used, with 5 misses resulting in termination of the acuity task.[58]

3.2.4 Wavefront aberration measurements

Residual on-axis ocular aberrations were measured at distance and near (40 cm) using a COAS-HD wavefront sensor (Johnson and Johnson, Santa Ana, CA) with a mirror assembly that allowed the subject to view a distant or near (40cm) target during measurement. To further assess

the effect of residual aberrations on word recognition and reading performance, two single value metrics were calculated.

Root mean square wavefront error (RMS) was quantified as the square root of sum of squares of the normalized Zernike coefficients for a 4mm pupil.[9] The visual image quality metric, log Visual Strehl Ratio (logVSX)[9,10] was also calculated from the residual aberration measurements for a 4mm pupil.

3.2.5 Corneal topography

Oculus Pentacam corneal topographer (Oculus Inc., Arlington, WA) was used to quantify the morphology of the cornea, and from the measurements disease severity was determined.

3.2.6 Experimental setup for word recognition

3.2.6.1 Positioning of the subjects

Subjects were seated and the head stabilized with a chin and forehead rest. The stimuli were presented on a gamma corrected miniature (11 cm in width * 6.5 cm in height) LCD monitor display (1920*1080 pixels) which is shown by the arrow in Figure 3.1.

Figure 3.1 The experimental set up for measuring word recognition ability at 40cm. The subject's task is to read the word presented on a miniature monitor display (indicated by the arrow). The subject had the ability to control the pace of the task, as word presentation speed was controlled via the subject keying of the space bar.

Individual words from the Stanford Question Answering Dataset (SQuAD)[59] were displayed to assess threshold word recognition. The words were chosen from the high frequency word list (2159 words). The words were presented with a cue ('+' indicating the words location at the center of the LCD monitor). The words were presented using a custom written python program (python.org) already in use in the laboratory of Dr. Daniel Coates.[60] The words were presented as black/gray text on a bright white background (350 cd/m2). The subject pressed the spacebar key to start each trial, allowing the subject to control the pace of the experiment and to rest any point as needed. A post-mask consisting of randomly scrambled letters was presented following the presentation of the test word. Figure 3.2 represents a trial for high contrast words without (figure 3.2A) and with (figure 3.2B) the presence of 4 flanking words.

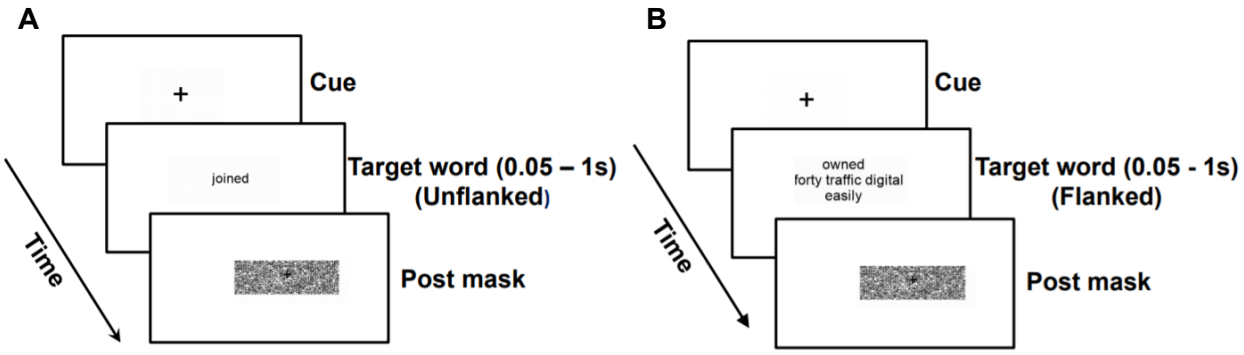

Figure 3.2 A representative trial consisting first of the appearance of a '+', which acted as a cue indicating the eventual location of the word. The individual words without (figure 3.2A) or with surrounding flanker words (figure3.2B) were presented from the SQuAD dataset (with varying font size, duration and contrast as described below). Following word presentation, a post mask appeared, consisting of scrambled letters scaled to the font sizes presented during the trial.

3.2.6.2 Stimulus conditions

For this experiment, the parameters that were varied included: 5 font sizes, 2 contrast levels, 5 durations of stimulus presentation and with or without 4 flanking words. Ten repeats with unique words (none of the individual words being presented more than once) at each font size, stimulus duration and contrast were presented in a randomized fashion for a total of 2000 trials (1000 trials/eye). Trials were divided into four blocks/eye based on the contrast levels and flankers condition). Duration and letter size varied within each block. Before the actual experiment, a block consisting of 50 trials was presented to familiarize each individual with the task. The specifics of each variable are as follows:

Font sizes: The letters for the words consisted of vertical height determined by the minimum angle of resolution subtended at 40cm. This was validated by comparing the vertical height of the letter on the screen to the printed, commercially available reading charts (Good-lite, Elgin, IL). The font size of the words presented were based on an individual's high or low contrast near visual acuity at the time of enrollment. Each individual viewed five different font sizes of Arial type. The five different font sizes for presenting individual word consists of words starting at a size defined by an individual's high/low contrast near visual acuity. An additional 4 sizes defined as one line below and one, two and three lines above the individual's visual acuity were also tested. Preliminary data suggested low contrast words were challenging to read for keratoconus subjects and three lines above low contrast acuity would not be adequate to determine threshold for word recognition in some subjects. Hence, we modified the paradigm for keratoconus subjects for the low contrast words to range from the individual's low contrast visual acuity level to 4 lines above their low contrast visual acuity level. Due to the physical limitations of our screen, the largest font size that could be tested was 1.1 logMAR at 40cm.

Stimulus durations: The words were presented at five different durations: 50, 125, 250, 500 and 1000 milliseconds.

Contrasts: Testing for all font sizes and durations was completed for both 100% Weber contrast and 25% Weber contrast.

Testing Order: The eye which would be tested first was randomized followed by randomization of 4 experimental blocks: high contrast unflanked, high contrast flanked, low contrast unflanked and low contrast flanked. Each block consisted of 250 words presented at 5 stimulus durations, 5 font sizes and each condition consisting of 10 repeats/trials.

Statistical analyses

Psychometric function were fitted using Palamedes toolbox[61] in Matlab software. The logistic function (PAL_Logistic) was used fo fit the data to determine the threshold.The slopes of the psychometric function, beta parameter were constrained between log20 to log25 to determine the minimum word acuity threshold. Paired t-test were done to compare the optical and visual performance between better and worse eyes.

3.3 Results

With a desire to represent performance encountered in the "real world" rather than a more optimized laboratory setting, individuals wore their habitual correction during data collection. For the individuals with keratoconus, 3 wore glasses, 1 wore soft contact lenses, 1 wore rigid-gas permeable lenses and 4 wore conventional scleral lenses. For the typically-sighted group, 1 subject wore glasses and the remaining subjects didn't wear any form of correction. The average age of the keratoconus subjects was 34 ± 12 and typically-sighted was 30.5 ± 9.4 years (*P*-value = 0.56). There were 5 males and 4 females in the keratoconus group and 4 males and 2 females

in the typically-sighted group. Based on the CLEK[62] classification, out of 18 eyes of 9 individuals with keratoconus, 5 eyes were mild (<45.0 D), 9 eyes were moderate (45.0 – 52.0 D) and 4 eyes (>52.0 D) were classified as severe keratoconus.

3.3.1 Residual higher-order aberrations and visual acuity measurements

All typically-sighted eyes were within the age-matched normal range for residual higher-order root mean square wavefront over a 4mm pupil and 14 out of the 18 eyes with keratoconus had elevated level of residual higher order aberration (> 0.183 microns).[2] Distance high contrast visual acuity and near high/low contrast visual acuity were also quantified to assess word recognition ability with respect to each subject's visual acuity that would be routinely quantified in the clinic. The results of these tests are summarized in Table 1 categorized by the "better" or "worse" eye, which was based on distance high contrast visual acuity. Example higher-order wavefront error maps, point spread functions and example psychometric functions were chosen based on the level of residual higher-order wavefront error for the eye as shown in Figure 3.3. As residual aberrations increase, the point spread function becomes less tightly focused and the psychometric functions tend to shift to the right, suggesting an increase in word recognition threshold (larger word sizes required to reach threshold).

Table 3.1 Summary of subject characteristics classified by "worse eye" and "better eye" where better and worse are based on distance high contrast visual acuity. As a general observation, individuals with keratoconus has poorer visual acuity (both high and low contrast) higher levels of HORMS and poorer values for logVSX than the typically-sighted subjects.

	Keratoconus subjects			**Typically-sighted subjects**		
	Mean ± SD			**Mean ± SD**		
	Worse Eye	**Better Eye**	**Mean Diff (*p*-value)**	**Worse Eye**	**Better Eye**	**Mean Diff (*p*-value)**
Distance HCVA	0.17 ± 0.22	0.00 ± 0.16	0.18 ± 0.18 (0.02)	-0.07 ± 0.09	-0.13 ± 0.10	0.06 ± 0.03 (0.003)
Near HCVA	0.21 ± 0.23	0.02 ± 0.13	0.19 ± 0.20 (0.02)	-0.06 ± 0.11	-0.13 ± 0.10	0.08 ± 0.13 (0.21)
Near LCVA	0.33 ± 0.28	0.08 ± 0.13	0.25 ± 0.26 (0.02)	-0.05 ± 0.11	-0.07 ± 0.07	0.01 ± 0.08 (0.69)
HORMS (μm)	0.42 ± 0.24	0.27 ± 0.10	0.19 ± 0.26 (0.06)	0.12 ± 0.04	0.14 ± 0.05	-0.02 ± 0.04 (0.19)
LogVSX	-1.34 ± 0.50	-1.05 ± 0.37	-0.29 ± 0.52	-1.00 ± 0.27	-0.64 ± 0.30	-0.36 ± 0.30

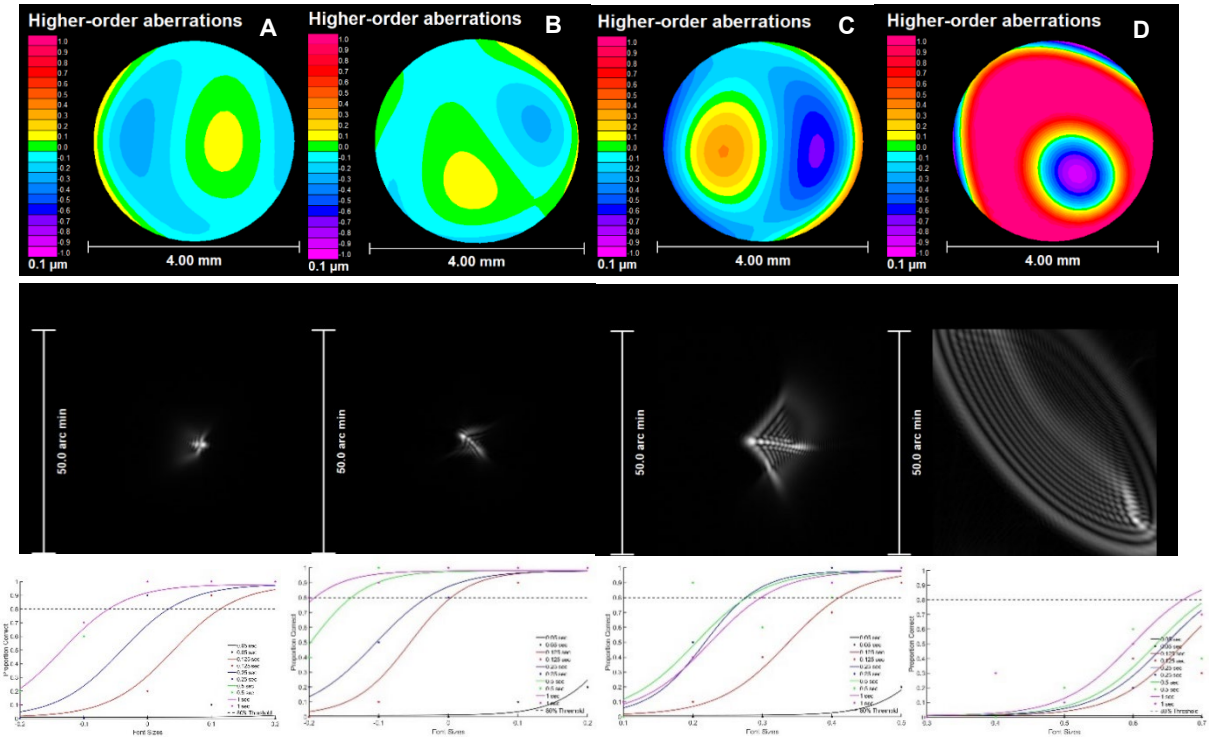

Figure 3.3 Examples representing residual higher-order wavefront error and point spread functions for A) a typically-sighted eye with median residual HORMS (0.14 µm). From the keratoconus sample, B) an eye with the lowest residual HORMS (0.09 µm) C) an eye with a level of aberration 0.34 µm near the medial sample (0.28 µm) and D) the eye with the largest residual HORMS (0.76 µm) in the keratoconus group are shown in top and middle panel. The bottom panel demonstrates representative psychometric functions for each of these conditions for 5 stimulus durations for unflanked high contrast words. X-axis represents font sizes in logMAR and Y-axis represent percentage correct. The horizontal dotted line is the 80% threshold.

3.3.2 Threshold word acuity as a function of stimulus durations

None of the eyes (typically-sighted or eyes with keratoconus) reached threshold for the 50-millisecond stimulus duration. Hence, thirty-two thresholds for word acuity based on stimulus duration, eye, presence or absence of flankers and high/low contrast were obtained for each individual (4 stimulus durations * 2 eyes * 2 flanking conditions * 2 contrasts). This resulted in a total of 288 thresholds data points for 18 eyes of 9 keratoconus and 192 threshold data points for 12 eyes of typically-sighted individuals.

When the threshold could be quantified for unflanked conditions but not for flanked conditions, extrapolation was performed to estimate the 80% correct threshold of the flanked condition. The method employed here was to calculate the 80% value from two data points obtained through the Palamedes algorithm, where both points were found above the 30% correct value on the psychometric function. Eleven of the 288 points (7 HC, 4 LC) were extrapolated in the keratoconus group and 3 of the 192 points (LC) were extrapolated in typically-sighted group. There were two instances where the threshold could not be obtained despite extrapolating the data. This occurred when subjects were better than 80% threshold at the starting acuity and therefore the psychometric function was essentially a flat line. Twelve out of 288 total thresholds (4 HC, 8 LC) in keratoconus group and 9 out of 192 total thresholds (4 HC, 5 LC) in typically-sighted individuals couldn't be determined because of a starting percentage correct greater than 80%. This also occurred when a subject had poor word recognition ability at a single duration, resulting in not obtaining two points above the 30% correct level. In these instances, extrapolations were not performed.

In addition, when the threshold couldn't be obtained in the unflanked condition, no extrapolation was performed for either unflanked or flanked conditions. Thirty-four out of 288 total thresholds

(6 pairs HC, 11 pairs LC) in the keratoconus group couldn't be determined because of inability to reach threshold for the unflanked condition as well as the flanked condition. Fourteen out of 17 pairs for the above-mentioned condition where threshold was not reached was for stimulus duration 125 and 250 milliseconds.

Figure 3.4 demonstrates the average threshold acuity for unflanked (A/B) and flanked (C/D) for both high contrast (A/C) and low contrast (B/D) conditions for the 18 keratoconus eyes and the 12 eyes of typically -sighted individuals. Figure 3.5 demonstrates the individual eye's threshold acuity for unflanked (A/B) and flanked (C/D) for both high contrast (A/C) and low contrast (B/D) conditions for the 18 keratoconus eyes and the 12 eyes of typically -sighted individuals.

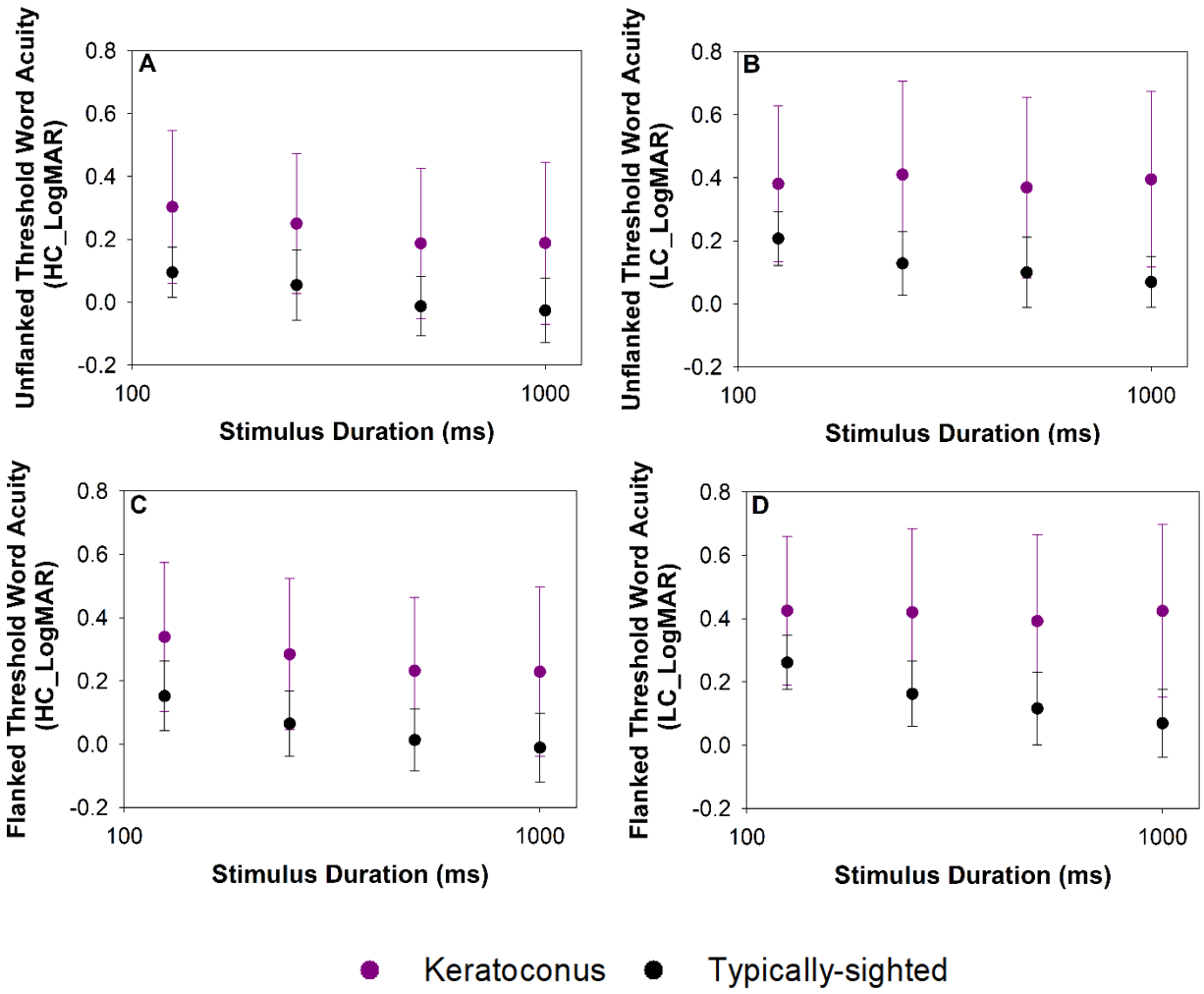

Figure 3.4 Average ±SD threshold word acuity were plotted as a function of stimulus durations (125ms, 250ms, 500ms and 1000ms) for unflanked (A/B) and flanked (C/D) conditions for both high contrast (A/C) and low contrast (B/D) words. Eyes with keratoconus (dark pink, filled circles) had greater variability (larger error bars) than typically-sighted individuals at all time points. Greater stimulus duration tended toward better threshold for typically-sighted individuals. In individuals with keratoconus, increase in duration tended toward better word acuity threshold for high contrast words, on average, with the low contrast thresholds remaining relatively unchanged.

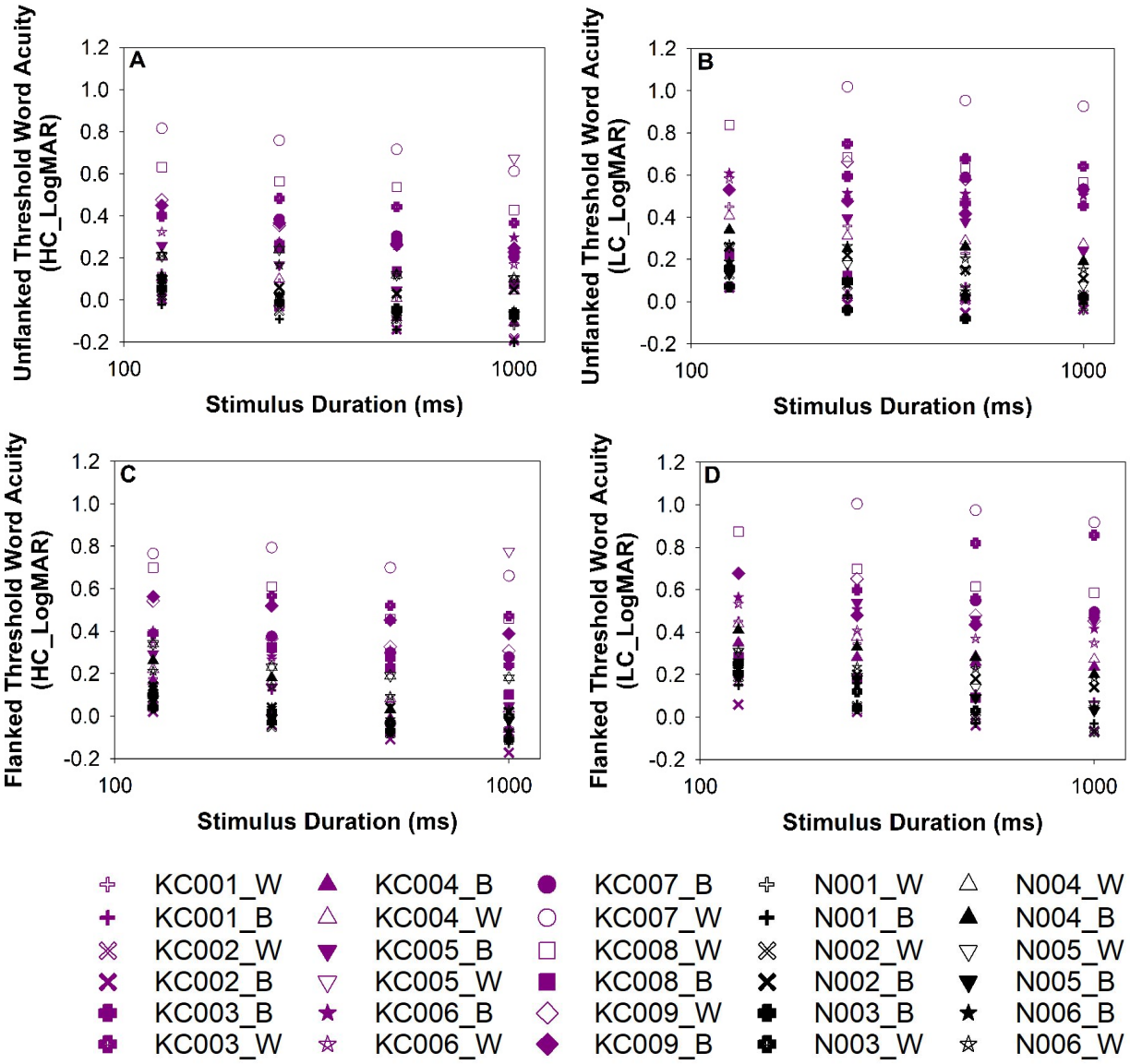

Figure 3.5 Individual datapoints for figure 3.4 are presented. Threshold word acuity were plotted as a function of stimulus durations (125ms, 250ms, 500ms and 1000ms) for unflanked (A/B) and flanked (C/D) conditions for both high contrast (A/C) and low contrast (B/D) words based on the better (filled symbols) and worse (unfilled symbols) eye. Eyes with keratoconus (dark pink) tended to have higher threshold values than typically-sighted individuals (black) at all timepoints.

3.3.3 Unflanked and flanked word acuity as a function of distance high contrast visual acuity and near high/low contrast visual acuity

Figures 3.6 show the actual threshold (solid filled circles) that were recorded and the extrapolated data points (unfilled stars). Figure 3.5 demonstrates the threshold acuity as a function of distant and near high contrast visual acuity for unflanked (A/B/C) and flanked (D/E/F) for high contrast (A/B/D/E) and low contrast (C/F) for 1000 millisecond stimulus duration for the 18 keratoconus eyes and the 12 eyes of typically -sighted individuals.

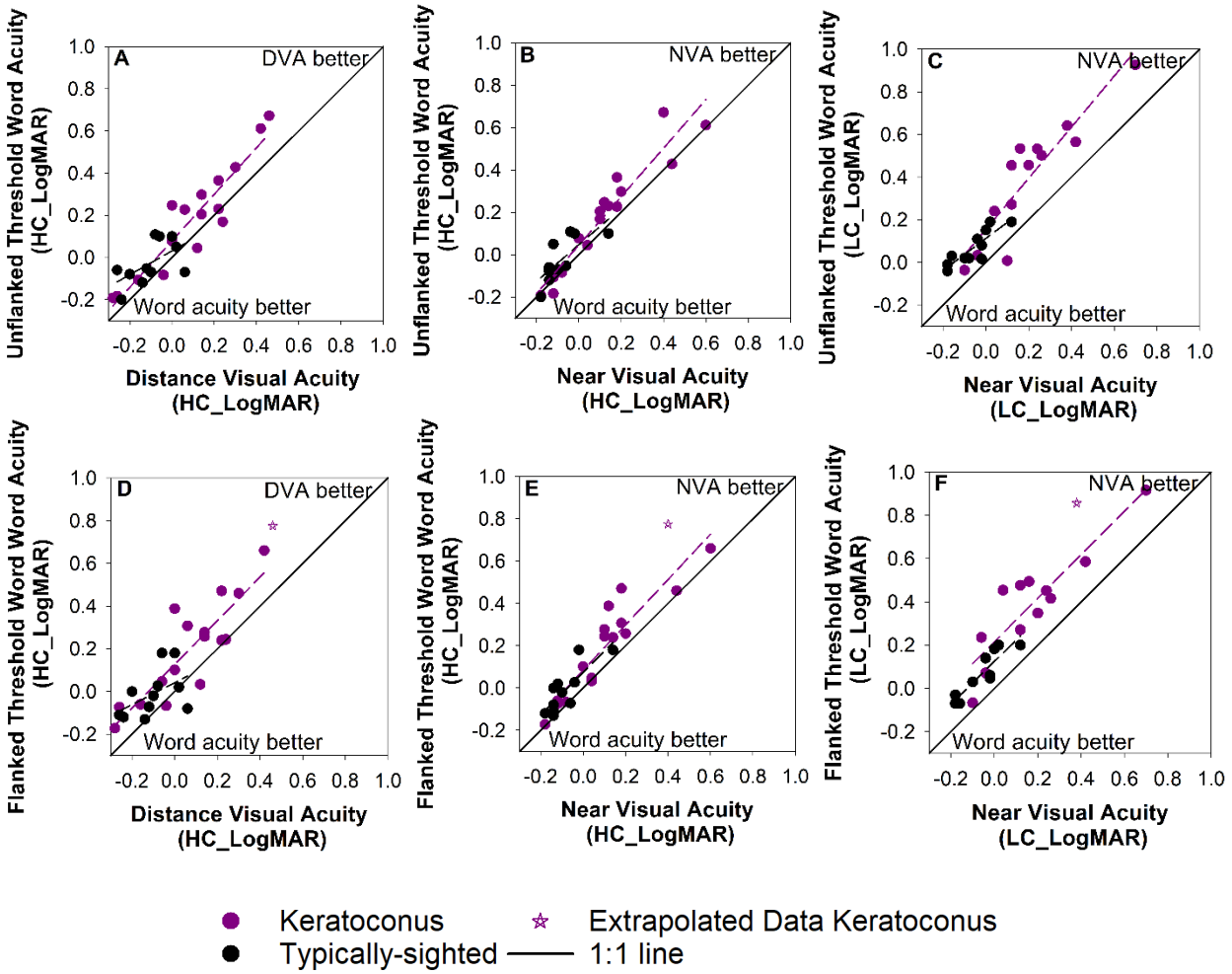

Figure 3.6 Threshold word acuity were plotted as a function of high contrast distance visual acuity and high/low contrast near visual acuity for unflanked (A/B/C) and flanked (D/E/F) conditions for both high contrast (A/B/D/E) and low contrast (C/F) words. In most cases, threshold word acuity was greater than visual acuity for both typically-sighted and individuals with keratoconus, more pronounced with low contrast words.

3.3.4 Unflanked and flanked threshold word acuity as a function of residual total wavefront error over a 4mm pupil

Figure 3.7 represents the unflanked (A/B) and flanked (C/D) threshold word acuity for 4 stimulus durations as a function of total residual wavefront error for a 4mm pupil for high contrast (A/C) and low contrast (B/D) words.

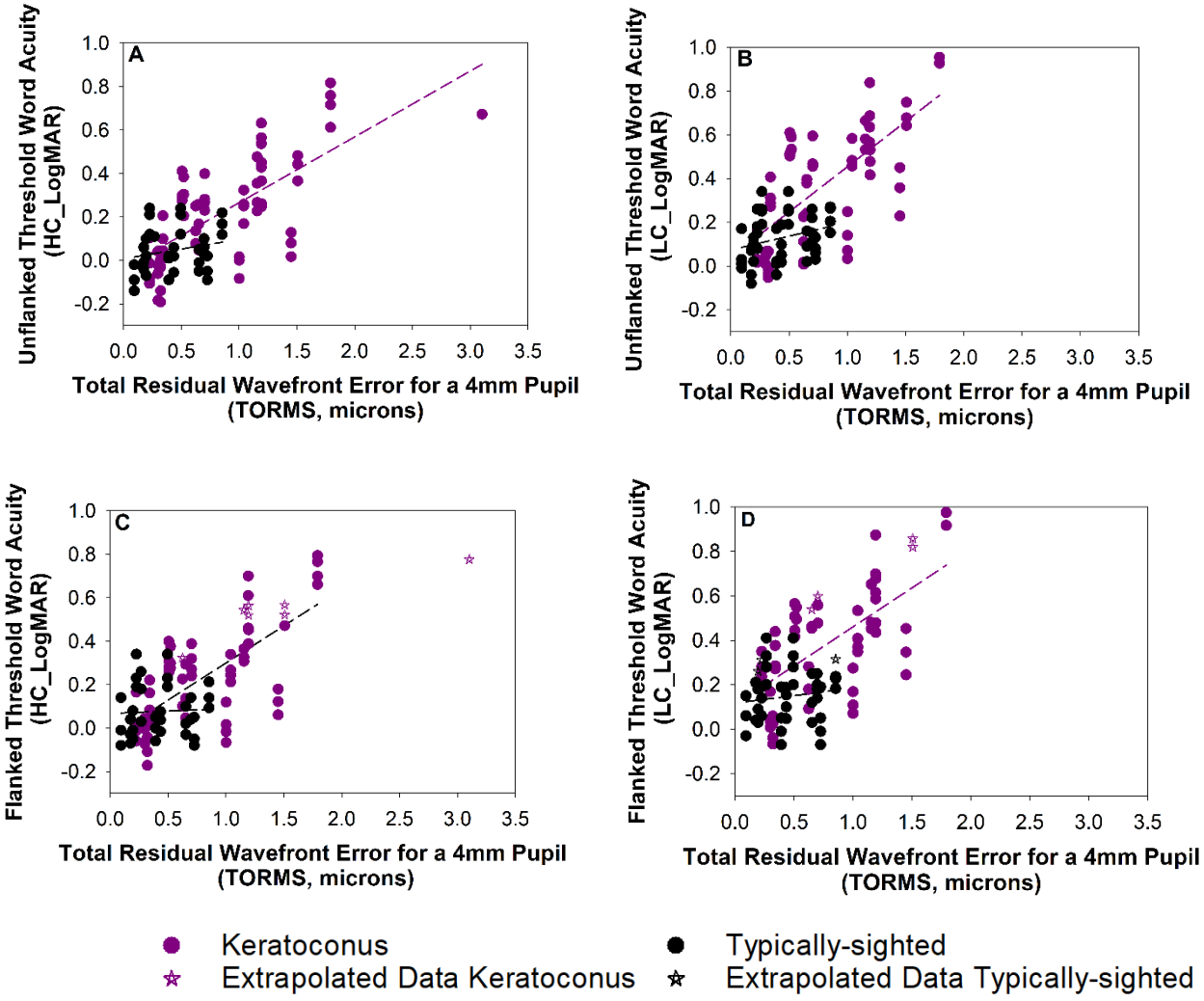

Figure 3.7 Threshold word acuity as a function of total residual wavefront error for a 4mm pupil were plotted for unflanked (A/B) and flanked (C/D) conditions for both high (A/C) and low contrast (B/D) words. With elevated residual wavefront error, there was a trend towards larger threshold for word recognition for individuals with keratoconus for both high and low contrast words.

3.3.5 Difference in threshold word recognition between two eyes

Figure 3.8 represents the differences between the worse and the better eye for unflanked (A/B) and flanked (C/D) conditions for both high (A/C) and low contrast (B/D) words.

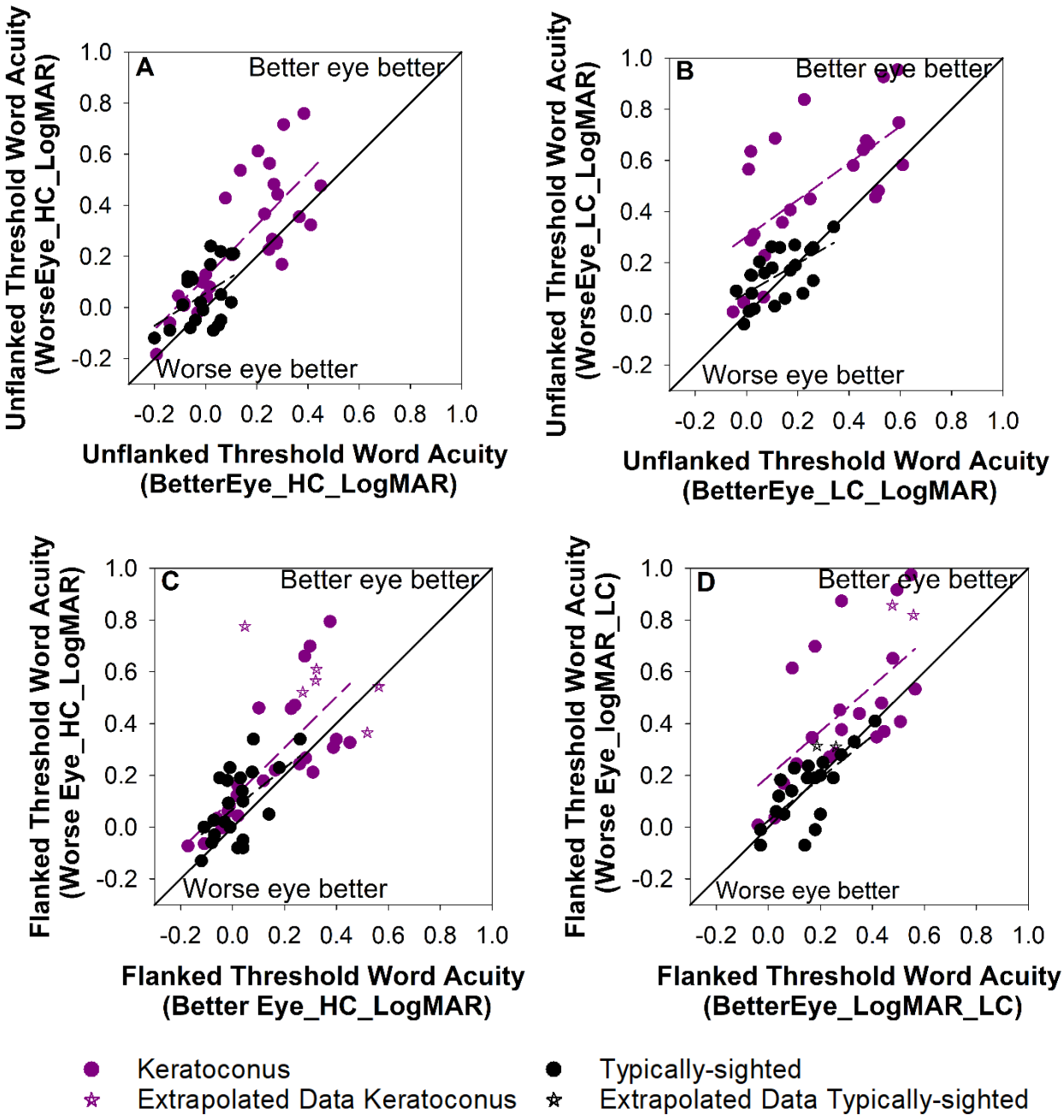

Figure 3.8 Worse/Better eye threshold word acuity were plotted for unflanked (A/B) and flanked (C/D) conditions for both high contrast (A/C) and low contrast (B/D) words. Threshold word acuity for the better eye were better than for the worse eye for individuals with keratoconus. With poor visual acuity, there was a trend towards larger difference between the two eyes. Typically-sighted individuals were close to the 1:1 line for both high and low contrast.

3.4 Discussion

High contrast distance visual acuity is often the single measure of visual function tested to determine visual performance in the clinic. It has been demonstrated that in cases where corneal irregularity exists, 20/20 visual acuity may not necessarily correlate to satisfactory visual performance.[14] This study considered this earlier finding in the context of real world tasks, which include reading single target words or words surrounded by other words representing basic units of reading performance at high (100%) or low (25%) contrast. The results suggested that individuals with keratoconus suffer reductions in performance, and that these reductions increase as the level of residual aberrations increase and that the individuals with keratoconus experience greater difference between eyes than typically-sighted individuals.

Interestingly, distance and near visual acuity (the clinical standard) could be quantified in all eyes studied, but threshold word acuity couldn't be quantified in all cases, even when words were scaled to the acuity level that was visible to the eye (subject) under test and were even presented at three to four lines above high/low contrast near visual acuity respectively. This suggests that the visual acuity task (which requires an individual to identify a single letter without any time pressure) may not represent the real-world challenges associated with tasks such as reading text.

Stimulus duration, which was increased from 50 to 1000 milliseconds during this experiment, did not alter the low contrast thresholds for individuals with keratoconus, suggesting that a duration of more than 1 second should be tested in future studies. This is an interesting finding as 1000 milliseconds (1second) stimulus duration is already roughly 3 times above the time

required for typically-sighted individuals to correctly read words.[63] This could be directly related to poor reading speed with increase in aberrations, which has been shown by Young et al.[55]

This study had several limitations. The logMAR step size was chosen to correspond to the step size that is employed on a logMAR acuity chart: 0.1. However, an alternative approach as commonly used in research while determining threshold visual acuity or contrast sensitivity could be using adaptive staircase method and searching more precisely around the minimum threshold. Three lines above high contrast near visual acuity were tested for high contrast and up to four lines above were tested for low contrast. These levels were large enough to quantify threshold based on the visual acuity for controls. All typically-sighted individuals were able to reach the 80% correct threshold, had enough points for extrapolation or were better than 80% threshold at the starting point. Using this paradigm clearly showed the challenges faced by clinicians and researchers when attempting to design experiments and collect data on individuals with keratoconus with a large range of residual aberrations. The paradigm that allowed for this large range failed to precisely quantify threshold word acuity when subjects were unable to read words at the given font sizes in keratoconus group because of the font size limitations.

The choice of display used to present stimulus was a miniature LCD display was made because if the high pixel density afforded by the camera (174.55 pixels/cm). This was chosen such that smaller words could be faithfully represented at the 40cm test distance. This choice lead to the limitations on the largest font size that could be tested in concert with flanking words.

Another limitation resulted from the decision to test a single font (Arial) which is built around the philosophy of proportional width. The effect of aberrations on fixed width letters and words were not quantified here. However, given the other variables of interest (contrast, duration,

flankers, visual angle) and the number of trials this demanded, limiting the current trials to a single font type seemed a reasonable first step.

Finally, reading is a binocular task and threshold word acuity was quantified monocularly in this study. This was done as keratoconus is an asymmetric disease and as a first step, it was important to quantify reading performance in the absence of binocularity, which would require consideration of neural processing. Future studies will include binocular performance and reading performance such as critical print size and reading speed.

In conclusion, word recognition thresholds were elevated compared to distance high contrast visual acuity. With longer duration, individuals with keratoconus showed improved high contrast acuity thresholds, but the effect was not seen in low contrast words, on average. There was a trend for greater threshold logMAR word acuity in individuals with elevated level of residual aberrations and asymmetry between word acuity thresholds between the better and worse eye for both high and low contrast words were more pronounced in keratoconus group.

Acknowledgments

The authors thank Hope Queener for use of the metrics calculation algorithm, which was developed partially through funding by the National Institutes of Health/National Eye Institute (P30 EY07551 (core grant to UHCO)). The authors also thank Krish Prahalad and Wei Hau Lew for help with the experimental setup for the reading. A portion of these findings were presented at the ARVO 2021 virtual meeting and submitted to present at American Academy of Optometry (AAO) 2021 annual meeting.

4 Chapter 4: Comparing the Camblobs2 contrast sensitivity test to the near Pelli-Robson contrast sensitivity test in normally-sighted young adults

Reprinted with modifications from: Rijal S, Cheng H, Marsack JD. Comparing the CamBlobs2 contrast sensitivity test to the near Pelli-Robson contrast sensitivity test in normally-sighted young adults. Ophthalmic Physiol Opt. 2021 (***In press***)

Appendix of this dissertation includes additional data and analyses of CamBlobs2, and Pelli-Robson contrast sensitivity collected on individuals with keratoconus. Those data were reported in Appendix because they were not part of the Ophthalmic and Physiological Optics publication.

4.1 Abstract

Purpose: Contrast sensitivity measurement has been proposed as a potential method for patients to assess their vision at home, between visits to their eye care professional. The CamBlobs2 contrast sensitivity test is one in a line of tests meant to be easily performed in the clinic or at home. The purpose of this study was to determine 1) the intra-visit coefficient of repeatability of the CamBlobs2 test to the near Pelli-Robson test and 2) the limits of agreement between these two tests on normally-sighted subjects.

Methods: Twenty-two normally-sighted subjects (mean age 28 ± 4 years) completed two instances each of the near Pelli-Robson and CamBlobs2 contrast sensitivity tests within a single study visit. Tests were performed monocularly on both eyes in a random order. Near Pelli-Robson tests were scored as 0.05 logCS for each letter correctly read after deducting the first triplet. CamBlob2 tests were scored as the highest contrast line where two or fewer blobs were correctly marked. The coefficient of repeatability was determined for both the near Pelli-Robson and CamBlobs2 tests as 1.96 times the standard deviation of the differences between the two measurements using the same type of chart on the same eye. The limits of agreement between the two tests were evaluated using Bland-Altman plots.

Results: The magnitude of mean difference between intra-visit measurements for both near Pelli-Robson and CamBlobs2 were less than 0.05 logCS and the coefficient of repeatability was within ± 0.20 logCS for both left and right eyes. The mean ± standard deviation differences between near Pelli-Robson and CamBlobs2 scores was -0.08 ± 0.08 (limits of agreement: -0.24 to 0.09) for right eyes and -0.05 ± 0.10 (limits of agreement: -0.23 to 0.14) logCS for left eyes based on average measurements.

Conclusions: The intra-visit repeatability of CamBlobs2 was consistent with the near Pelli-Robson contrast sensitivity test (± 0.20 logCS). With a 0.05 correction, the CamBlobs2 scores showed an excellent agreement with those of the near Pelli-Robson contrast sensitivity test.

Key points

1. The CamBlobs2 test, a disposable paper chart requires no maintenance, has multiple versions and can be administered at a habitual working distance.

2. In a normally-sighted sample of young adults, repeatability of the CamBlobs2 test was similar to that of the near Pelli-Robson test.

3. Given the fact that the CamBlobs2 test can be administered with minimal clinician involvement, it has the potential for at-home disease monitoring.

4.2 Introduction

While high contrast distance visual acuity is the most common and universally accepted test of visual performance, the results of this type of vision test do not reflect the full spectrum of visual characteristics important to an individual's experience in everyday life.[64] Real world visual experience is not restricted to high contrast visual targets, rather it is a combination of both high and low contrast visual stimuli. High contrast visual acuity is resistant to the presence of elevated higher order aberrations. For instance, in a study by Ravikumar et al.[12] it was shown that on average, there were six just noticeable differences in visual image quality (changes in visual percept that could be identified by an individual) before one line of high contrast visual acuity was lost. Another example of the limitation of high contrast visual acuity to reflect patient-perceived visual quality can be found in the "20/20 unhappy" clinical patient, which is defined as a patient that can accurately read the letters on the 20/20 line, but remains unhappy with their qualitative visual percept.[14] In cases of ocular disease, the discrepancies between high contrast distance visual acuity measured in the clinic and patient-perceived visual quality by an individual in the "real world" can lead to dissonance between the patients' percept of the quality of their vision and care providers' percept of their disease burden.[65]

One method to address the limitations of high contrast visual acuity is to employ additional visual tests that challenge aspects of the patient's percept that are left untested by high contrast visual acuity. One such category of tests is found in the quantification of an individual's ability to detect decreasing levels of contrast. Contrast is defined as the relative difference in luminance between a target and the background,[15] and threshold contrast is defined as the lowest contrast required to see a target reliably. Poor contrast sensitivity degrades the quality of vision by

reducing one's ability to distinguish objects from their background, affecting day to day activities, even in individuals with typical levels of visual acuity.[66] The impact of reduced contrast sensitivity can manifest in situations such as rain, fog or night driving, and contrast sensitivity tests have been used to evaluate patients with diseases such as glaucoma,[67,68] diabetes,[69,70] age-related macular degeneration,[71,72] amblyopia,[73,74] keratoconus,[6,43] and in assessing quality of vision after refractive surgeries,[75] to name a few.

There are several chart- and computer-based tests that can determine contrast sensitivity.[76–78] The Pelli-Robson letter contrast sensitivity chart is widely used in research settings to assess contrast sensitivity.[78,79] This contrast test is designed to measure threshold contrast for identification of a fixed size target letter. [38,76,80] The test is used as a reference standard for evaluating new contrast sensitivity charts.[78,79,81,82]

Pelli-Robson contrast sensitivity is not tested routinely in clinical practice. In addition, the Pelli-Robson contrast sensitivity chart itself needs careful handling to preserve the integrity of the chart. Therefore, it is not suitable for administering at home, which would be beneficial in situations where patients are suffering from a progressive disease and are asked by their clinicians to pay close attention to small changes in their perceived visual quality (example use of Amsler grid in AMD). Further, the clinical utility of repeated contrast sensitivity testing is hampered by the fact that charts (regardless of the test chosen) are only available in a handful of versions, making repeated testing prone to patient memorization of the letter ordering.

While the computer tablet-based tests such as iPad Contrast Sensitivity Test (https://www.ridgevue.com/)[79] and ClinicCSF (https://www.test-eye.com/en/)[78] address some of the shortcomings of the Pelli-Robson test like the need for careful handling and storage, they are

expensive, need supervision to perform the testing and cannot be easily administered in home settings. In an effort to address these challenges, Dr. John Robson (of Pelli-Robson) developed a new form of contrast testing, known throughout its evolutionary development by several names.[81–83] The version of this test under evaluation here is the CamBlobs2 (Precision Vision, Woodstock, IL), which was designed to be an inexpensive alternative for patients to self-monitor their disease progression and to remove barriers that have traditionally kept clinicians from assessing contrast sensitivity. The single-use paper chart can be self-administered by the patients at their habitual reading distances, and has multiple versions (12 in total) making it useful for repeated testing and monitoring longitudinal change in contrast sensitivity.[83–85]The CamBlobs2 contrast sensitivity chart has an advantage of new design where the test consists of one line with 4 blobs randomly located and change in contrast between lines in step size of 0.05 logCS, instead of 3 letters of the same contrast in a step of 0.15 logCS for Pelli- Robson ,[76] and 0.04 logCS per letter for MARS contrast sensitivity test.[77] The disposable paper chart requires no maintenance and the spot design provides stable contrast sensitivity for a large photopic luminance range.[86]

Testing contrast sensitivity in normally-sighted individuals that are habitually corrected provides insight as to how the individual performs in the real world, with their habitual correction. Thus, the results from this study represent how the individual would perform in day to day life, rather than with an optimized correction that is provided simply for the experiment. Given the goal of testing patients with their habitual correction, aberration data, as well as visual image quality data are also recorded to ensure the patients are not operating at an extreme optical deficit, and are experiencing typical performance for their age. This study assessed the within session reliability of the CamBlobs2 contrast sensitivity chart and near Pelli-Robson contrast sensitivity chart in normally-sighted, habitually corrected individuals. In addition, the limits of agreement

between CamBlobs2 contrast sensitivity scores and near Pelli-Robson contrast sensitivity scores were also quantified.

4.3 Methods

All procedures adhered to the tenets of the Declaration of Helsinki. All experimental protocols were approved by the Institutional Review Board at the University of Houston. Prior to testing, all subjects signed an informed consent document after a thorough explanation of the experimental protocol and an opportunity to discuss any questions about the protocol and potential risks.

4.3.1 Subjects

Twenty-two normally-sighted individuals, aged 28 ± 4 years (range: 22 to 33 years, female: male = 12:10) completed the study. Seven individuals were habitual soft contact lens wearers and the remaining 15 did not habitually wear refractive correction. All subjects completed testing in their habitual refractive state. To be included in the study, all subjects had to demonstrate habitual high contrast visual acuity of 20/25 or better. Individuals enrolled in the study were free of ocular disease, had no prior ocular surgeries and no systemic illness which would be expected to impact visual performance.

4.3.2 Accommodation measurements

As the CamBlobs2 and near Pelli-Robson tests are administered at near, subjective accommodative amplitude was assessed with the push-up technique to ensure subjects had an accommodative amplitude sufficient for the stimulus demand at 40 cm (+ 2.5 D).

4.3.3 Wavefront measurements

Distance wavefront measurements were recorded to ensure the optical performance of the eyes under test were representative of the normally-sighted population at large. Measurements were recorded with a COAS HD wavefront sensor (Johnson & Johnson Vision, Santa Ana, CA), with the subject's natural pupil in dim room illumination as subjects focused the fellow eye on a distant target. For each measurement, the instrument was aligned to the eye under test, the subject was asked to blink and then hold their eyes open during measurement. Aberration measurements were described by a 10th radial order normalized Zernike polynomial fit.[87] Three measurements were recorded on each eye and a custom MATLAB program was used to mathematically average the coefficients of the three measurements over the largest common pupil size determined via pupilometry during visual function testing.[5,6] The distance wavefront measurements were rescaled to 4mm pupil diameter[34] for pooling, and higher-order root mean square wavefront error (HORMS)[9] was calculated for the 3rd – 6th radial orders. The visual image quality metric visual Strehl ratio (VSX)[9] was also calculated over a 4mm pupil. In order to compare with VSX values available for typical individuals in the literature,[10] an optimal refraction was first identified and applied prior to VSX calculation (the same method utilized in the normative dataset). The values for both HORMS and optimized VSX were compared to typical values available in literature.

4.3.4 Visual function testing

All participants completed two instances each of the visual performance tests described below. Visual performance testing was performed monocularly on both eyes, in random order (6

measurements randomized within the eye and also the order of the eyes was randomized) at natural pupil size with habitual correction.

4.3.4.1 Distance visual acuity

Four unique (2 per eye) Early Treatment Diabetic Retinopathy Study logMAR charts were displayed with black letters on a white background (Display++ monitor; Cambridge Research Systems, Kent, United Kingdom) and a background luminance of 116 cd/m2 (Minolta LS-110; Konica Minolta, Ramsey, NJ) at a distance of 4 meters. Each chart consisted of 13 rows of 5 letters, where each letter was given a value of 0.02 logMAR. A letter-by-letter scoring method was used, in which each letter read correctly up to the fifth miss[58]was used to determine visual acuity. The readings obtained from the two unique charts were averaged.

4.3.4.2 Near Pelli-Robson Contrast sensitivity test

The near Pelli-Robson contrast sensitivity test (Precision Vision, Woodstock, IL) was used as the gold standard in this study. Near Pelli-Robson is a smaller version (angle subtended by each letter is 2.29 degrees at 40cm) of the original Pelli-Robson chart for testing at reading distance. Near Pelli-Robson contrast sensitivity test consists of multiple lines of fixed size Sloan letters arranged into two columns of triplets.[76,80,88]Letters in each triplet have the same contrast. Contrast is reduced in each successive triplet by 0.15 log unit or a factor of $1/\sqrt{2}$. The contrast sensitivity measurement ranges from a high contrast (0.00 logCS) to a low contrast (2.25 logCS). The chart was set per the recommended guidelines at 40 cm test distance with a luminance of 93 cd/m2 with overhead room lighting. The subjects read the chart from the top and the test was terminated when two letters in a triplet were missed. Contrast sensitivity was scored by counting each letter read correctly as 0.05 log unit and deducting 0.15 for the first triplet.

4.3.4.3 CamBlobs2 contrast sensitivity test

The CamBlobs2 contrast sensitivity test[83–85,89] (Precision Vision, Woodstock, IL) consists of 25 rows (0.85 to 2.05 logCS, 14% to 0.9% Weber contrast) with 4 round grey blobs of 9 mm diameter (77 minutes at 40 cm) in each row. Each blob in the same row has the same contrast and the contrast in successive row reduces by 0.05 log units, equivalent to a single letter in a near Pelli-Robson chart. There are 12 (A-L) test versions, each with a transparency overlay used to correctly score the chart. Per the instructions provided by the manufacturer, this test could be performed at habitual working distance in a room illumination with flexibility for the subject to tip/tilt the chart. As near Pelli-Robson was to be placed exactly at 40cm, for comparison the CamBlobs2 chart was placed at 40cm, and the subject was allowed to tip/tilt the chart when attempting to identify the targets to comply with the instructions. This is consistent with the fact that individuals are allowed to tip/tilt their heads during Pelli-Robson contrast sensitivity testing. Luminance on the chart was 91 cd/m2. The subjects were asked to mark the position of each blob starting from the top (darker) to bottom (less dark) of the chart. The topmost row where there were no more than two blobs correctly marked determined the log contrast sensitivity. Figure 1 demonstrates the administration and scoring of the CamBlobs2 Chart. Three additional scoring methods were also explored to assess limits of agreement. The first subtracted the blobs that were missed from the contrast sensitivity measured using the above mentioned protocol. The second denied credit for the top most line where there were two or fewer blobs correctly marked. The third combined the first and second approaches, deducted the blobs missed from the approach that denied credit for the top most line where there were two or fewer blobs correctly marked. A value of 0.0125 was subtracted for each missed blob.

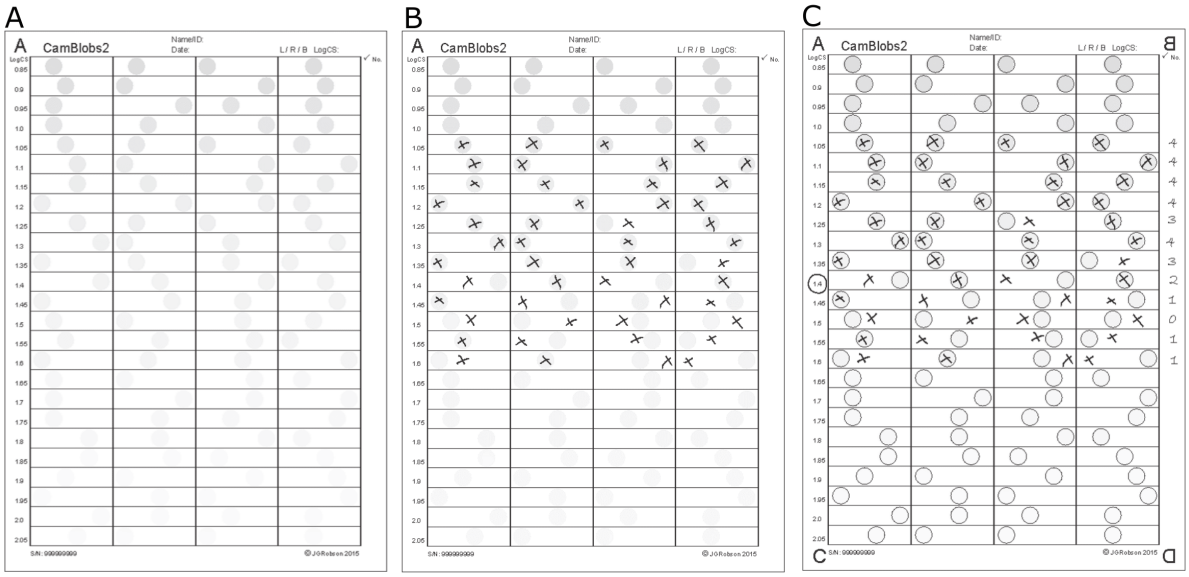

Figure 4.1 (A) The CamBlobs2 chart, (B) administration of the test by a subject and (C) scoring to determine contrast sensitivity. The subjects were asked to mark the position of all the four blobs in each row until they could no longer see the blobs. An overlay template (shown in C) was then placed over the chart for scoring. The topmost line which had two or fewer blobs correctly marked determined contrast sensitivity (1.4 log unit in the example shown)

Statistical Analyses

Bland-Altman plots were used to evaluate the intra-visit repeatability of each contrast sensitivity test and the agreement between two tests.[90] The difference of the two paired measurements were plotted against the mean of the two measurements. A linear regression was performed between the difference and the mean to check the assumption that the difference did not vary systemically over the range of measurement. Out of the 8 linear regressions performed (see r2 and p-value in Figure 2&3), only one showed a p value < 0.05 (Figure 2D) despite a weak coefficient of determination (r2 = 0.3). This likely reflects an increased Type I error associated with multiple comparisons (the probability of discovering a false-positive result = $1-(1-0.05)^8 = 0.34$).

The intra-visit coefficient of repeatability was determined for both the near Pelli-Robson and CamBlobs2 contrast sensitivity test as 1.96 times the standard deviation of the differences between the two measurements using the same type of chart on the same eye.

The limits of agreement between the near Pelli-Robson and CamBlobs2 were calculated using 1.96 times the standard deviation of the differences between the measures of the two tests.38

4.4 Results

The data of right and left eyes are presented separately throughout. All data for right eyes in the graphs are represented by black filled circles and all the data for left eyes are represented by black diamonds. In the case of overlapping data points, the X-axis data are shifted by a small amount (± 0.01 logCS) to ensure all data points are visible. These shifts are not incorporated into the numerical results.

4.4.1 Residual higher-order aberrations and visual acuity measurements

One of the challenges of testing visual performance with the habitual correction (rather than a refraction that is optimized for the experiment) is that the individual may experience a high amount of residual uncorrected refractive error. To guard against this, wavefront aberration data and visual image quality were calculated. The results of these calculations demonstrate that the cohort of habitually-corrected individuals is performing at a level consistent with typical subjects. Visual acuity, higher order root mean square wavefront error (HORMS) and optimized visual Strehl ratio (VSX) for the study sample were recorded and compared to typical values in an effort to assess whether the sample could be considered typical. The results of these tests are

summarized in Table 4.1. The eyes had optical performance (HORMS), visual image quality (VSX) and visual performance (logMAR visual acuity) typical for their age.

Table 4.1 Sample Characteristics

Measurements	**Right Eyes**	**Left Eyes**	**Normative Data**
Residual HORMS (4mm pupil)	0.116 ± 0.035	0.129 ± 0.079	0.100 ± 0.044[2]
Distance high contrast visual acuity (logMAR)	-0.12 ± 0.10	-0.12 ± 0.09	-0.07 ± 0.05[13]
VSX (4mm pupil)	0.619 ± 0.145	0.636 ± 0.159	0.576 ± 0.125[10]

4.4.2 Intra-visit repeatability of near Pelli-Robson and CamBlobs2 contrast sensitivity tests

The magnitude of mean difference between intra-visit measurements were less than 0.05 logCS for both near Pelli-Robson and CamBlobs2 contrast sensitivity tests. The coefficient of repeatability was ± 0.18 for right eyes and ± 0.20 for left eyes (Figure 4.2 A&B) for near Pelli-Robson scores. The coefficient of repeatability was ± 0.14 for right eyes and ± 0.18 for left eyes (Figure 4.2 C&D) for CamBlobs2 scores. Average scores for both test and re-test for both eyes are listed in Table 4.2 and intra-visit 95% limits for logCS are listed in Table 4.3.

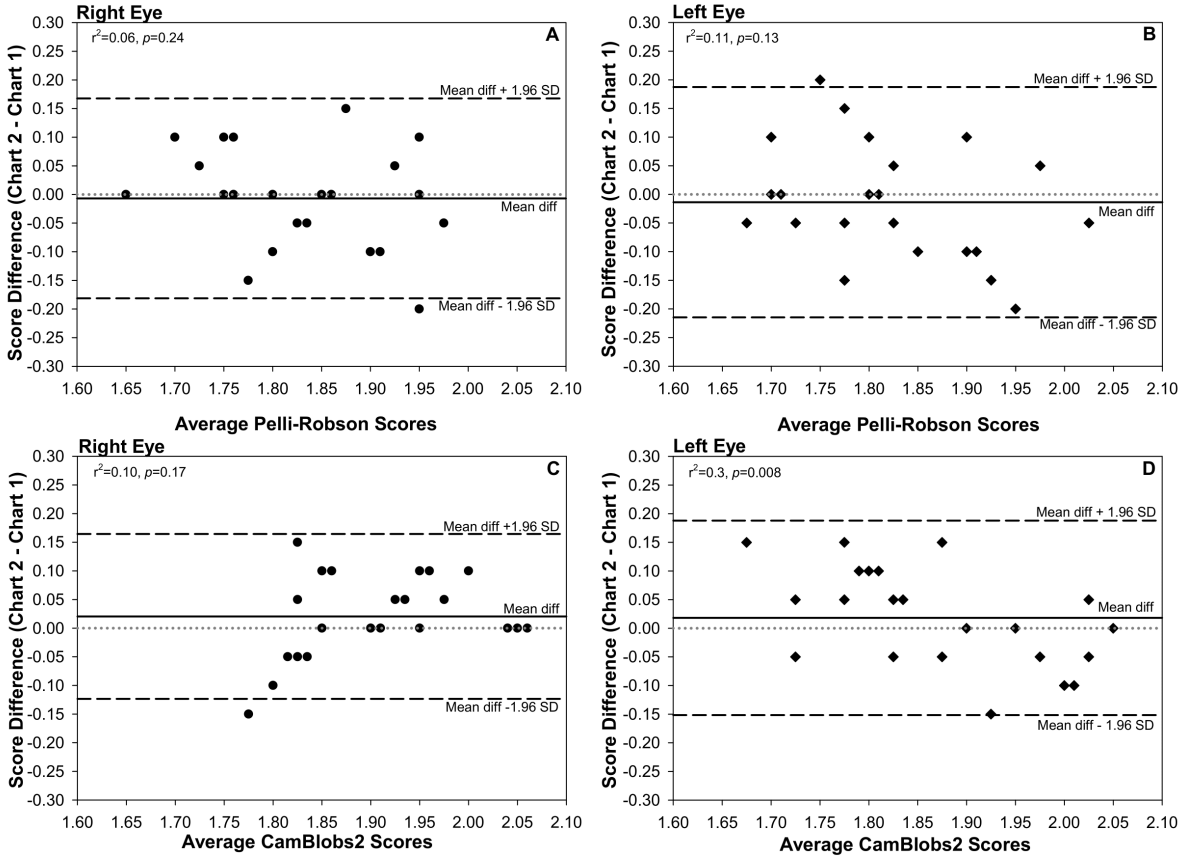

Figure 4.2 Bland-Altman plot for intra-visit near Pelli-Robson (top panel A and B) and CamBlobs2 (bottom panel C and D) scores in right eye and left eye. The magnitude of mean difference ± standard deviation between the intra-visit measurements was -0.01 ± 0.09 logCS for right eye and -0.01 ± 0.10 logCS for left eye for near Pelli-Robson scores. The magnitude of mean difference ± standard deviation between the intra-visit measurements was 0.02 ± 0.07 logCS for right eye and 0.02 ± 0.09 logCS for left eye for CamBlobs2 Scores.

Table 4.2 Mean ± standard deviation logCS for intra-visit measurements

		Right Eyes **Mean ± SD**	**Left Eyes** **Mean ± SD**
Near Pelli-Robson	Test 1	1.83 ± 0.11	1.83 ± 0.12
	Test 2	1.83 ± 0.09	1.81 ± 0.10
CamBlobs2	Test 1	1.89 ± 0.08	1.86 ± 0.14
	Test 2	1.91 ± 0.10	1.88 ± 0.09

For the seven individuals wearing soft contact lenses, the average contrast sensitivity for near Pelli-Robson was OD: 1.80 ± 0.09, OS: 1.78 ± 0.07 and CamBlobs2 contrast sensitivity was OD: 1.88 ± 0.09, OS: 1.81 ± 0.13. All the seven contact lens-wearing subjects had levels of contrast sensitivity considered typical (OD: 1.84 ± 0.12, OS: 1.81 ± 0.13)[80] for the age range.

Table 4.3 Intra-visit 95% limit for logCS (mean +/-1.96 SD of differences)

	Right Eyes	**Left Eyes**
	95% LoA	**95% LoA**
Near Pelli-Robson test 1 vs test 2	-0.01 ± 0.18	-0.01 ± 0.20
CamBlobs2 test 1 vs test 2	0.02 ± 0.14	0.02 ± 0.18
CamBlobs2 vs near Pelli-Robson (single)	-0.08 ± 0.22	-0.05 ± 0.20
CamBlobs2 vs near Pelli-Robson (average)	-0.08 ± 0.16	-0.05 ± 0.20

4.4.3 Limits of agreement between near Pelli-Robson and CamBlobs2 contrast sensitivity

The mean ± standard deviation difference between near Pelli-Robson and CamBlobs2 scores was -0.08 ± 0.11 (LoA: 0.13 to -0.30) for right eyes and -0.05 ± 0.10 (LoA: 0.15 to -0.26) logCS for left eyes when compared with the randomly chosen one of the two replicates for each test as shown in Figure 4.3.

The mean ± standard deviation difference between near Pelli-Robson and CamBlobs2 scores was -0.08 ± 0.08 (LoA: 0.09 to -0.25) for right eyes and -0.05 ± 0.10 (LoA: 0.14 to -0.24) logCS for left eyes when compared with the average of the two measurements for each test as shown in Figure 4.3.

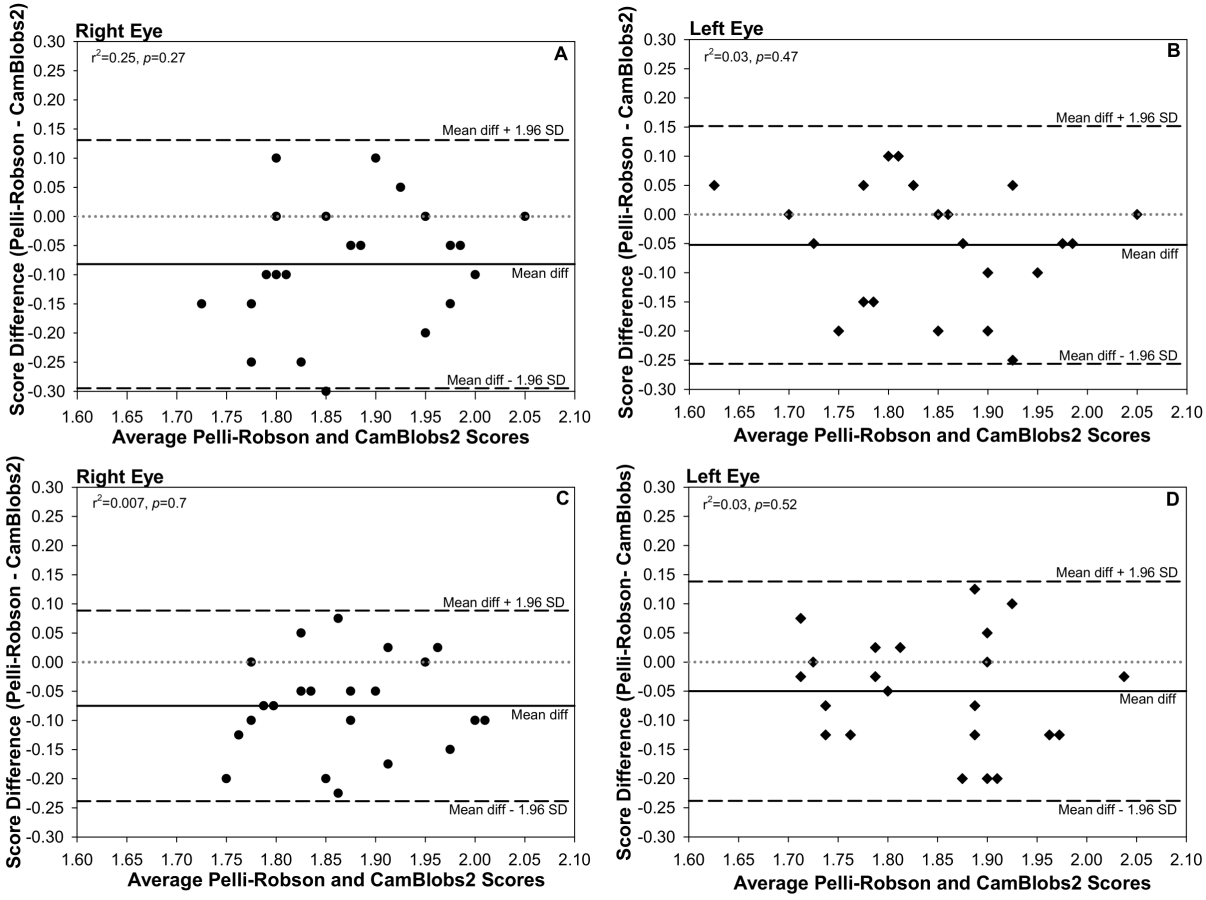

Figure 4.3 Bland-Altman plot for agreement between CamBlobs2 and Pell-Robson. The magnitude of mean difference ± standard deviation between the intra-visit measurements was -0.08 ± 0.11 logCS in right eye and -0.05 ± 0.10 logCS in left eye for single measurement (top panel A and B). The magnitude of mean difference ± standard deviation between the intra-visit measurements was -0.08 ± 0.08 logCS in right eye and -0.05 ± 0.10 logCS in left eye for average measurements (bottom panel C and D).

4.4.4 Assessing repeatability and limits of agreement with additional scoring methods

All three methods led to improvement in the agreement between CamBlobs2 and near Pelli-Robson contrast sensitivity to a bias very close to 0 as shown in Table 4. However none of the scoring methods improved repeatability of the CamBlobs2 test (columns 1 and 3 in Table 4.4) beyond what was observed for the original scoring method (Table 4.3).

Table 4.4 Intra-visit 95% limit for logCS (mean +/-1.96 SD of differences) with three different scoring methods between repeated administration of CamBlobs2 charts (columns 1,3) and between CamBlobs2 and near Pelli-Robson (2,4).

	Right Eyes		**Left Eyes**	
	95% LoA		**95% LoA**	
	CamBlobs2 test 1 vs test 2	CamBlobs2 vs Near Pelli-Robson	CamBlobs2 test 1 vs test 2	CamBlobs2 vs Near Pelli-Robson
Method 1: subtract 0.0125 for each missed blob	0.02 ± 0.16	-0.04 ± 0.17	0.02 ± 0.14	0.00 ± 0.19
Method 2: must get 3 or more correct per line	0.02 ± 0.14	-0.03 ± 0.16	0.02 ± 0.18	0.00 ± 0.19
Method 3: must get 3 or more correct and subtract 0.0125 for each missed blob	0.02 ± 0.16	-0.01 ± 0.16	0.01 ± 0.14	0.01 ± 0.19

4.5 Discussion

Visual impairment is commonly assessed based on the standard high contrast visual acuity task.[91] But this test, used in isolation, may be insensitive to aspects of the visual percept that are important to an individual. Incorporating additional visual performance measures, such as measures of contrast sensitivity, may increase our clinical insight into the true impact of disease burden on an individual. An inexpensive, self –administrable, disposable paper chart such as the CamBlobs2 contrast sensitivity tes[83–85,89] would enable more widespread use of contrast testing. When compared to the commonly used test near Pelli-Robson contrast sensitivity test, the intra-visit repeatability of CamBlobs2 was similar if not slightly better. A repeatability of ≤ 0.20 units, or 4 letters (on the near Pelli-Robson) or 4 lines (on the CamBlobs2), is consistent with the repeatability found in other studies.[77,79,82]

On this cohort of normally-sighted individuals, the average difference across all eyes between the two tests was (0.062), approximately one letter (0.05 logCS) as measured by the near Pelli-Robson test. The limits of agreement between the two tests is within the repeatability of each test (± 0.20 logCS).

The additional scoring methods explore the equivalence of the two charts, there is no definitive reason to suppose that the estimated contrast sensitivity should be the same for near Pelli-Robson and CamBlobs2 (both because of the nature of the task and the scoring system used). While it may well be the case that one can choose a scoring system that balances out the difference in difficulty of the task (as demonstrated in Table 4.4), the best scoring system is not the one that demonstrates equivalence with a different scoring system, but the one that gives the lowest variability. While the performance of the two tests is similar, they were achieved on two very

different types of visual tasks. One is a letter recognition task and the other is a detection task. The design of the CamBlobs2 chart has been shown to be more resistant to small changes in test distance than letter-based charts.[84] The results suggest that the CamBlobs2 chart (or its successor, the SpotChecks) could be used in place of the near Pelli-Robson chart. SpotChecks are similar to Camblobs2 contrast sensitivity chart. Dr. John Robson made this test with finer steps of contrast of 0.01 logCS instead of 0.05 logCS as in CamBlobs2. CamBlobs2 is available on request but commercially Spotchecks are available to measure contrast with smaller step size.

While the CamBlobs2 test is an intuitive, not requiring literacy, easy to perform task, it is likely that the individual will have never performed such a task in the past. Given the fact that the test comes in 12 versions, making memorization of any given chart impossible, the individual being tested may find it helpful to undergo a test run to become familiar with the task.

This study has several limitations. One limitation arose from a limitation of the near Pelli-Robson test itself, which has a limited number of versions (3) of the test. We used the three available near Pelli-Robson contrast sensitivity chart versions for test-retest for each eye. One of the charts was randomly repeated to allow a total of 4 tests (2 tests on each of 2 eyes). This could lead to a potential learning effect, but this is unlikely as the near Pelli-Robson tests were interleaved with all other vision tests performed, reducing the likelihood of letter order memorization. Our study subjects had a narrow age range (22 to 33 years). All of these measurements have been made on normally-sighted subjects and there is no guarantee that subjects with compromised vision would show the same result. Though these kind of tests have the potential to be helpful for patients to self-monitor changes that could be indicative of disease progression in between office visits, no home administration testing was completed as part of

this study. Also, the multiple versions of CamBlobs2 was useful to test intra-visit repeatability, we did not assess temporal stability which could be a potential benefit as camBlobs2 is available in multiple versions. One general limitation of using both CamBlobs2 and Pelli-Robson contrast sensitivity test was that the overall contrast sensitivity function could not be tested.

In conclusion, with recent focus of medicine on individual care, quality of vision and overall quality of life, tests like CamBlobs2 which can be administered while the patient is waiting, without active clinician's involvement, are encouraging to quickly assess visual function beyond high contrast acuity. The test also provides results that are repeatable, and consistent with the near Pelli-Robson contrast sensitivity test. With a 0.05 correction, the CamBlobs2 scores showed an excellent agreement with those of the near Pelli-Robson contrast sensitivity test.

Acknowledgments

The authors would like to thank Dr. John Robson for permission to use Figure 1, for providing the CamBlobs2 charts used in the study and for providing his scientific feedback on a draft of this manuscript. The authors thank Dr. Larry Thibos, Dr. Raymond Applegate, Dr. Gareth Hastings and Hope Queener for use of the metrics calculation algorithm, which was developed partially through funding by the National Institutes of Health/National Eye Institute (P30 EY07551 (core grant to UHCO)). A portion of these findings were presented at the American Academy of Optometry (AAO) 2020 virtual meeting.

5 Chapter 5: Summary and future directions

This dissertation explored the manner in which typically-sighted individuals and individuals with keratoconus perform simulated, clinical and real-world visual tasks under varying levels of uncorrected optical aberration. Individuals with keratoconus have elevated levels of both lower- and higher-order aberrations[3–7] and therefore individuals from this population serve as an ideal subject base for assessing the impact of aberrations on visual performance. It is a well-established fact that elevated levels of uncorrected optical aberrations lead to poor visual function. Hence, our aim was not to quantify the loss in performance in uncorrected eyes, but rather assess the level of optical and visual performance when people were wearing their best habitual refractive correction or simulated optimized correction (simulating their real-world experience). In an effort to make the results from this dissertation more generalizable, both individuals with keratoconus and typically-sighted individuals were included in this study. Individual chapter reflections are discussed below:

5.1 Chapter 2: The impact of misaligned wavefront-guided correction in a scleral lens for the highly aberrated eye

Customized wavefront-guided scleral lenses target elevated residual higher-order aberrations.[4–6] Studies have shown that on average, wavefront-guided scleral lenses provide superior visual acuity, contrast sensitivity, and visual image quality compared to the conventional scleral lenses.[4–6] The front surface optical design of a wavefront lenses requires information through a well-fitted scleral lens and the on eye translation data. Wavefront-guided correction performs ideally when registered to the underlying wavefront error. Conventional scleral lenses serve as a vehicle for carrying wavefront-guided correction and hence, the amount of decentration becomes important when designing a wavefront-guided correction. Based on the inferior and temporal

displacement of the conventional scleral lenses with respect to the pupil center, wavefront-guided correction is displaced superior and nasally to align with the pupil center. It adds complexity as the scleral lenses are decentered by different magnitude in each eye based on the shape of the cone, action of eyelids, contour of the sclera to name a few. Quantification of these misalignment data is not a part of common clinical practice. The measurements forms yet another technical barrier to the delivery of wavefront-guided corrections. Hence, this study tested the viability of common rather than individualized decentered locations. Average decentered location was defined as the mean and the horizontal vertical translations of the conventional scleral lenses in 36 eyes of 18 individuals with keratoconus. The simulated performance at this location was compared to the simulated performance at the geometric center of the lens and the simulated performance at the pupil center. The results of this study suggested that the loss in simulated performance due to this over-simplification would not be worth over the benefit provided by the well-aligned wavefront-guided correction.

Some of the limitations of the study were first the optical and visual performance through wavefront-guided corrected were simulated rather than measured on-eye. The findings of this study were not confirmed by designing wavefront-guided corrections at non-pupil centered locations for the eyes of real individuals. In addition, the potential effects of rotation were not considered. This was done purposely to separate the sole effects of translation as it is one of the important contributors affecting the optics of a wavefront guided correction. Finally, the three-letter test-retest reliability was used as a threshold to assess whether recommendation could be made to design wavefront-guided correction at one of the the non-pupil centered locations. Though 17 of the 36 eyes fell at or below the threshold suggesting these eyes could potentially benefit from the simplification of the fitting process. However, we were not able to isolate the

characteristics of the eyes which benefitted, and which did not. A previous study had used stochastic parallel gradient descent (SPGD) algorithm[40] to optimize the partial-magnitude correction for eyes with keratoconus based on the scleral lens movement. Future direction includes using machine learning algorithms with information about the residual aberrations, lens translations, cut-off thresholds incorporated to identify the determining factors which lead to different amount of loss in performance.

5.2 Chapter 3: Word recognition thresholds as a function of disease severity in keratoconus

Higher-order aberrations are elevated in individuals with keratoconus despite current state of art corrections.[7] Subjective questionnaires used to measure quality of life have shown that quality of life is reduced in keratoconus [54,92] and reading is one of the important factors leading to reduced quality of life and the level of reduction in reading ability is a function of disease severity.[53] It is concerning as there is a degree of asymmetry present in the eyes with keratoconus and the disease is progressive in nature. An individual who is enjoying a good quality of life at a young age may experience reduced quality of life if the disease progresses. It is hypothesized that high contrast visual acuity alone might not be enough to describe sophisticated tasks like word recognition and reading. The presence of dioptric blur and individual lower- and higher-order aberrations have shown to affect word recognition[50] and reading performance uniquely.[49,55] With a range of disease severity, the optical and visual performance in the population with keratoconus could vary from being equivalent to the typically-sighted individuals to a significantly reduced level. The findings from the study demonstrated that there is a reduction in performance associated with severity.

Based on the number of repeats required and the step size of 0.1 logMAR, the levels of font sizes that could be tested were limited. We tested up to three lines above near high contrast acuity for high contrast words and up to four lines above near low contrast acuity for low contrast words. One alternative approach for future studies could be using adaptive staircase methods to identify thresholds, which would utilize a finer search near the threshold. We also tested threshold word acuity monocularly and since reading is performed binocularly, future studies could focus on quantifying binocular word acuity threshold and how they correlate to monocular word acuity thresholds. Word acuity was assessed here with and without flankers. Using flankers is a simplified representation of words that would look like in a page of text. Going further, it would be useful to assess reading performance (speed, critical print size, maximum reading speed, eye movements, oral versus silent reading) in individuals with keratoconus as it has been suggested that even if aberrations don't make the words illegible, they might reduce reading speed.[55]

5.3 Chapter 4: Comparing the CamBlobs2 contrast sensitivity test to the near Pelli-Robson contrast sensitivity test in the typically-sighted adults

Our world consists of not just high contrast, but a mixture of contrast ranging from high to low. In a typical clinical environment, the preferred method for testing visual performance is distance high contrast letter acuity. Visual acuity describes the quantity of the image but provides limited information about the quality of the image. It has been shown that before there is 1 line loss in acuity, there is on average, six steps change in visual image quality which is the percept identified by an individual[93] and not all people who achieve 20/20 vision are happy patients.[14] Contrast sensitivity tests provide additional information about the quality of image and there are numerous paper based[76,77] and electronic charts[78,79] that can be used to measure the full contrast

sensitivity function or a threshold for particular spatial frequency. Some of the limitations of these tests are they have stringent installation and scoring criteria, depend strongly on illumination, testing distance and require active clinician' s involvement. To address these challenges Dr. John Robson (of Pelli-Robson) designed a new contrast sensitivity test called the CamBlobs2[83–85] contrast sensitivity test with an advantage of a new design (blobs rather than letters). This test needs minimal clinician's involvement, less dependent on luminance.[86] The intra-visit repeatability and limits of agreement of the CamBlobs2 contrast sensitivity test were compared with near Pelli-Robson contrast sensitivity test in habitually-corrected typically-sighted individuals and individuals with keratoconus. The intra-visit repeatability of the CamBlobs2 was similar to near Pelli-Robson test with a mean bias close to 0.0 and had good agreement between two charts with a 0.05 bias correction in habitually corrected typically-sighted individuals.

Some of the limitations of the study were the decision to test a limited age range that consisted of relatively young subjects. Future directions could include testing contrast sensitivity in a home-based setting, using modified versions of the disc target to assess other spatial frequencies and identifying the mechanisms associated with blob detection.

6 Appendix

Comparing the CamBlobs2 contrast sensitivity test to the near Pelli-Robson contrast sensitivity test in keratoconus individuals

6.1 Methods

6.1.1 Subjects

Seven habitually-corrected individuals with keratoconus, aged 34.86 ± 12.88 years (range: 22 to 51 years, female: male = 5:2) completed the study. One individual wore habitual soft contact lens and the remaining 6 wore scleral lenses.

The rest of the methodology was the same as Chapter 4.

6.2 Results

All keratoconus subjects had a certain degree of asymmetry in their OD/OS aberration structures and the sample size was small for this dataset. Therefore, all data for right eyes and left eyes are pooled and presented in a single graph. Consistent with the results from Chapter 4 for the typically- sighted cohort, in the case of overlapping data points, the X-axis data are shifted by a small amount (± 0.01 logCS) to ensure all data points are visible. These shifts are not incorporated into the numerical results.

6.2.1 Residual higher-order aberrations and visual acuity measurements

Table 6.1 Sample characteristics

Measurements	Worse Eyes	Better Eyes	Normative Data
Residual HORMS (4mm pupil)	0.485 ± 0.284	0.190 ± 0.311	0.100 ± 0.044[2]
Distance high contrast visual acuity (logMAR)	0.24 ± 0.22	0.03 ± 0.09	-0.07 ± 0.05[13]

6.2.2 Intra-visit repeatability of near Pelli-Robson and CamBlobs2 contrast sensitivity tests

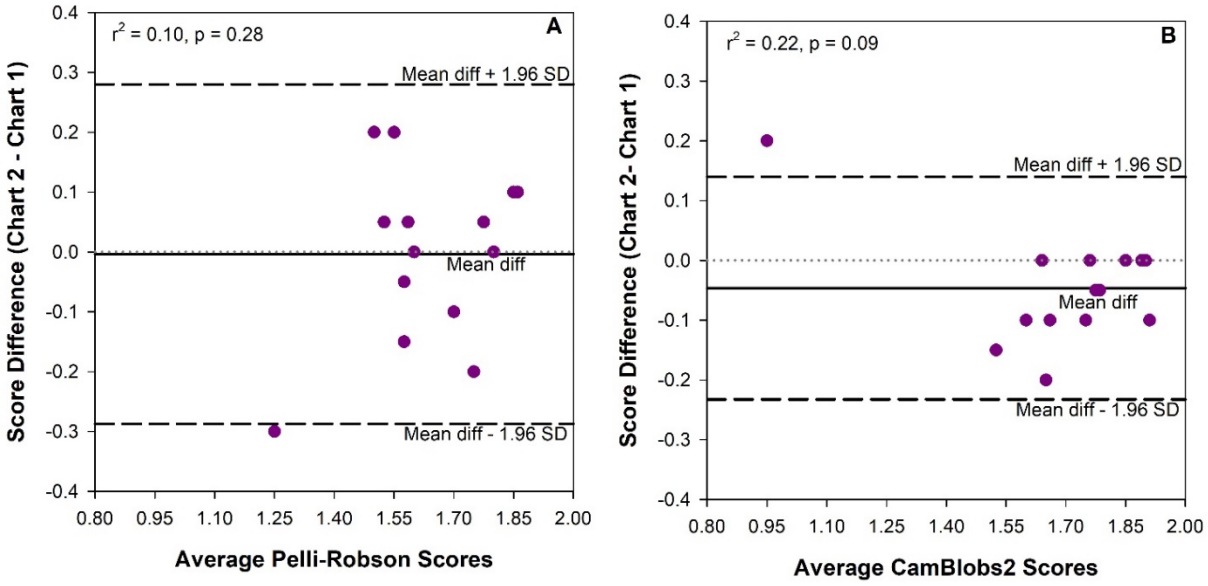

Figure 6.1 Bland-Altman plot for intra-visit Pelli-Robson (Figure 6.1A) and CamBlobs2 (Figure 6.2 B) scores in individuals with keratoconus. The magnitude of mean difference ± standard deviation between the intra-visit measurements was 0.00 ± 0.14 logCS for Pelli-Robson and -0.05 ± 0.09 logCS for CamBlobs2 scores.

Table 6.2 Mean ± standard deviation logCS for intra-visit measurements

		Mean ± SD
Near Pelli-Robson	Test 1	1.64 ± 0.16
	Test 2	1.63 ± 0.20
CamBlobs2	Test 1	1.71 ± 0.27
	Test 2	1.67 ± 0.22

Table 6.3 Intra-visit 95% limit for logCS (mean +/-1.96 SD of differences)

	95% LoA
Near Pelli-Robson test 1 vs test 2	0.00 ± 0.28
CamBlobs2 test 1 vs test 2	-0.05 ± 0.19
CamBlobs2 vs near Pelli-Robson (single)	-0.03 ± 0.37
CamBlobs2 vs near Pelli-Robson (average)	-0.05 ± 0.28

6.2.3 Limits of agreement between near Pelli-Robson and CamBlobs2 contrast sensitivity

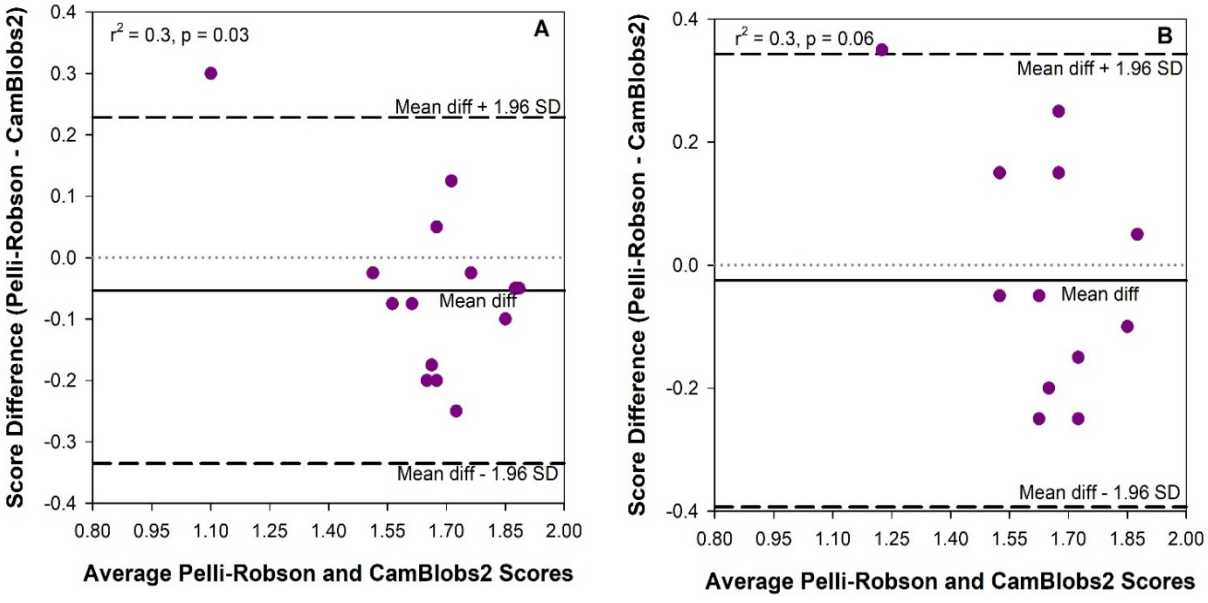

Figure 6.2 Bland-Altman plots for agreement between CamBlobs2 and Pell-Robson tests in individuals with keratoconus. The magnitude of mean difference ± standard deviation between the two tests were -0.05 ± 0.14 logCS for average measurements (Figure 6.2 A) and -0.03 ± 0.19 logCS for single measurement (Figure 6.2 B).

6.2.4 Assessing repeatability and limits of agreement to additional scoring methods

Table 6.4 Intra-visit 95% limit for logCS (mean +/-1.96 SD of differences) with three different scoring methods between repeated administration of CamBlobs2 charts (column 1) and between CamBlobs2 and near Pelli-Robson (column 2).

	95% LoA	
	CamBlobs2 test 1 vs test 2	CamBlobs2 vs Near Pelli-Robson
Method 1: subtract 0.0125 for each missed blob	-0.04 ± 0.17	-0.01 ± 0.28
Method 2: must get 3 or more correct per line	-0.05 ± 0.19	0.00 ± 0.28
Method 3: must get 3 or more correct and subtract 0.0125 for each missed blob	-0.04 ± 0.17	0.04 ± 0.28

InterpretationThe repeatability was within ± 0.30 logCS for both the tests and the limit of agreement between near Pelli-Robson and CamBlobs2 scores was -0.05 ± 0.28 for average measurements and -0.03 ± 0.19 logCS for single measurement.

6.3 Visual performance data for 4 keratoconus subjects common to Experiments in Chapters 3 and 4.

Four of the seven keratoconus subjects included in the CamBlobs2 study (Chapter 4) were also the part of the reading study (Chapter 3). Table 6.5 shows the data for visual acuity, contrast sensitivity, reading threshold for both unflanked and flanked words (1000 millisecond stimulus duration) for both high and low contrast. It shows that contrast sensitivity is reduced in subjects with poor visual acuity and reading thresholds are elevated with low contrast. These subject numbers are low, and more data is needed to assess the significance of these observations.

Table 6.5 Summary of visual acuity, contrast sensitivity scores for both near Pelli-Robson and CamBlobs2 scores and threshold word acuity for four individuals with keratoconus

ID	Eye	D_VA (HC)	Contrast	N_VA	UF_WA	FL_WA	PR	CamBlob
KC4	RE	0.14	HC	0.1	0.20	0.28	1.55	1.65
			LC	0.16	0.53	0.49		
	LE	0.42	HC	0.6	0.61	0.66	1.60	1.52
			LC	0.70	0.93	0.92		
KC5	RE	0.30	HC	0.44	0.43	0.46	1.60	1.85
			LC	0.42	0.56	0.58		
	LE	0.00	HC	0	0.08	0.10	1.80	1.90
			LC	0.1	0.01	Higher than threshold		
KC6	RE	-0.06	HC	0.04	Higher than threshold	0.05	1.75	1.77
			LC	0.04	0.24	0.45		
	LE	0.46	HC	0.4	0.67	0.77	1.25	0.95
			LC	0.80	Didn't reach threshold	Didn't reach threshold		
KC7	RE	0.06	HC	0.18	0.23	0.31	1.57	1.77
			LC	0.24	0.53	0.45		
	LE	0.00	HC	0.12	0.25	0.39	1.57	1.75
			LC	0.22	Higher than threshold	Higher than threshold		

7 References

1. Rabinowitz YS. Keratoconus. Surv Ophthalmol 1998;42:297–319.

2. Salmon TO, van de Pol C. Normal-eye Zernike coefficients and root-mean-square wavefront errors. J Cataract Refract Surg 2006;32:2064–74.

3. Marsack JD, Parker KE, Pesudovs K, Donnelly WJ, Applegate RA. Uncorrected wavefront error and visual performance during RGP wear in keratoconus. Optom Vis Sci 2007;84:463–70.

4. Sabesan R, Johns L, Tomashevskaya O, Jacobs DS, Rosenthal P, Yoon G. Wavefront-Guided Scleral Lens Prosthetic Device for Keratoconus. Optom Vis Sci 2013;90:314–23.

5. Marsack JD, Ravikumar A, Nguyen C, Ticak A, Koenig DE, Elswick JD, Applegate RA. Wavefront-Guided Scleral Lens Correction in Keratoconus. Optom Vis Sci 2014;91:1221–30.

6. Hastings GD, Applegate RA, Nguyen LC, Kauffman MJ, Hemmati RT, Marsack JD. Comparison of Wavefront-guided and Best Conventional Scleral Lenses after Habituation in Eyes with Corneal Ectasia. Optom Vis Sci 2019;96:238–47.

7. Rijal S, Hastings GD, Nguyen LC, Kauffman MJ, Applegate RA, Marsack JD. The Impact of Misaligned Wavefront-guided Correction in a Scleral Lens for the Highly Aberrated Eye. Optom Vis Sci 2020;97:732–40.

8. Thibos LN, Applegate RA, Schwiegerling JT, Webb R, VSIA Standards Taskforce Members. Vision science and its applications. Standards for reporting the optical aberrations of eyes. J Refract Surg 2002;18:S652-60.

9. Thibos LN, Hong X, Bradley A, Applegate RA. Accuracy and precision of objective refraction from wavefront aberrations. J Vis 2004;4:9–9.

10. Hastings GD, Marsack JD, Thibos LN, Applegate RA. Normative best-corrected values of the visual image quality metric VSX as a function of age and pupil size. J Opt Soc Am Opt Image Sci Vis 2018;35:732–9.

11. Hastings GD, Marsack JD, Thibos LN, Applegate RA. Combining optical and neural components in physiological visual image quality metrics as functions of luminance and age. J Vis 2020;20:20.

12. Ravikumar A, Marsack JD, Bedell HE, Shi Y, Applegate RA. Change in visual acuity is well correlated with change in image-quality metrics for both normal and keratoconic wavefront errors. J Vis 2013;13:28–28.

13. Hastings GD, Marsack JD, Nguyen LC, Cheng H, Applegate RA. Is an objective refraction optimised using the visual Strehl ratio better than a subjective refraction? Ophthalmic Physiol Opt 2017;37:317–25.

14. Nguyen LC, Kauffman MJ, Hastings GD, Applegate RA, Marsack JD. Case Report: What Are We Doing for Our "20/20 Unhappy" Scleral Lens Patients? Optom Vis Sci 2020;97:826–30.

15. Pelli DG, Bex P. Measuring contrast sensitivity. Vision Res 2013;90:10–4.

16. Applegate RA, Marsack JD, Ramos R, Sarver EJ. Interaction between aberrations to improve or reduce visual performance. J Cataract Refract Surg 2003;29:1487–95.

17. Kennedy RH, Bourne WM, Dyer JA. A 48-year clinical and epidemiologic study of keratoconus. Am J Ophthalmol 1986;101:267–73.

18. Godefrooij DA, de Wit GA, Uiterwaal CS, Imhof SM, Wisse RPL. Age-specific Incidence and Prevalence of Keratoconus: A Nationwide Registration Study. Am J Ophthalmol 2017;175:169–72.

19. Zadnik K, Barr JT, Edrington TB, Everett DF, Jameson M, McMahon TT, Shin JA, Sterling JL, Wagner H, Gordon MO. Baseline findings in the Collaborative Longitudinal Evaluation of Keratoconus (CLEK) Study. Invest Ophthalmol Vis Sci 1998;39:2537–46.

20. Schornack MM. Scleral lenses: a literature review. Eye Contact Lens 2015;41:3–11.

21. Rathi VM, Mandathara PS, Taneja M, Dumpati S, Sangwan VS. Scleral lens for keratoconus: technology update. Clin Ophthalmol 2015;9:2013–8.

22. Jinabhai AN. Customised aberration-controlling corrections for keratoconic patients using contact lenses. Clin Exp Optom 2020;103:31–43.

23. Visser E-S, Van der Linden BJJJ, Otten HM, Van der Lelij A, Visser R. Medical Applications and Outcomes of Bitangential Scleral Lenses: Optom Vis Sci 2013;90:1078–85.

24. Ticak A, Marsack JD, Koenig DE, Ravikumar A, Shi Y, Nguyen LC, Applegate RA. A Comparision of Three Methods to Increase Scleral Contact Lens On-eye Stability. Eye Contact Lens 2015;41:386–90.

25. Vincent SJ, Alonso-Caneiro D, Collins MJ. The temporal dynamics of miniscleral contact lenses: Central corneal clearance and centration. Cont Lens Anterior Eye 2018;41:162–8.

26. Vincent SJ, Collins MJ. A topographical method to quantify scleral contact lens decentration. Cont Lens Anterior Eye 2019;42:462–6.

27. Vincent SJ, Fadel D. Optical considerations for scleral contact lenses: A review. Cont Lens Anterior Eye 2019;42:598–613.

28. Kowalski LP, Collins MJ, Vincent SJ. Scleral lens centration: The influence of centre thickness, scleral topography, and apical clearance. Cont Lens Anterior Eye 2020;43:562–7.

29. Guirao A, Williams DR, Cox IG. Effect of rotation and translation on the expected benefit of an ideal method to correct the eye's higher-order aberrations. J Opt Soc Am Opt Image Sci Vis 2001;18:1003–15.

30. Shi Y, Applegate RA, Wei X, Ravikumar A, Bedell HE. Registration Tolerance of a Custom Correction to Maintain Visual Acuity: Optom Vis Sci 2013;90:1370–84.

31. Guirao A, Cox IG, Williams DR. Method for optimizing the correction of the eye's higher-order aberrations in the presence of decentrations. J Opt Soc Am Opt Image Sci Vis 2002;19:126–8.

32. de Brabander J, Chateau N, Marin G, Lopez-Gil N, Van Der Worp E, Benito A. Simulated optical performance of custom wavefront soft contact lenses for keratoconus. Optom Vis Sci 2003;80:637–43.

33. Yoon G, Jeong TM. Effect of the movement of customized contact lens on visual benefit in abnormal eyes. J Vis 2003;3:38–38.

34. Dai G. Wavefront Optics for Vision Correction. 2008.

35. Applegate RA, Sarver EJ, Khemsara V. Are all aberrations equal? J Refract Surg 2002;18:S556-62.

36. McLellan JS, Prieto PM, Marcos S, Burns SA. Effects of interactions among wave aberrations on optical image quality. Vision Res 2006;46:3009–16.

37. Marsack JD, Thibos LN, Applegate RA. Metrics of optical quality derived from wave aberrations predict visual performance. J Vis 2004;4:8–8.

38. Elliott DB, Yang KC, Whitaker D. Visual acuity changes throughout adulthood in normal, healthy eyes: seeing beyond 6/6. Optom Vis Sci 1995;72:186–91.

39. Raasch TW, Bailey IL, Bullimore MA. Repeatability of Visual Acuity Measurement: Optom Vis Sci 1998;75:342–8.

40. Shi Y, Queener HM, Marsack JD, Ravikumar A, Bedell HE, Applegate RA. Optimizing wavefront-guided corrections for highly aberrated eyes in the presence of registration uncertainty. J Vis 2013;13.

41. Hastings GD, Zanayed JZ, Nguyen LC, Applegate RA, Marsack JD. Do Polymer Coatings Change the Aberrations of Conventional and Wavefront-guided Scleral Lenses?: Optom Vis Sci 2020;97:28–35.

42. Kniestedt C, Stamper RL. Visual acuity and its measurement. Ophthalmol Clin N Am 2003;16:155–70.

43. Puri S, Bhattarai D, Adhikari P, Shrestha JB, Paudel N. Burden of ocular and visual disorders among pupils in special schools in Nepal. Arch Dis Child 2015;100:834–7.

44. Bhattarai D, Gnyawali S, Silwal A, Puri S, Shrestha A, Kunwar MB, Upadhyay MP. Student-led screening of school children for refractive error correction. Ophthalmic Epidemiol 2018;25:133–9.

45. Whittaker SG, Lovie-Kitchin J. Visual requirements for reading. Optom Vis Sci 1993;70:54–65.

46. Primativo S, Spinelli D, Zoccolotti P, De Luca M, Martelli M. Perceptual and Cognitive Factors Imposing "Speed Limits" on Reading Rate: A Study with the Rapid Serial Visual Presentation. Paterson K, ed. PLoS ONE 2016;11:e0153786.

47. Chung STL, Legge GE, Pelli DG, Yu C. Visual factors in reading. Vision Res 2019;161:60–2.

48. Chung STL, Mansfield JS, Legge GE. Psychophysics of reading. XVIII. The effect of print size on reading speed in normal peripheral vision. Vision Res 1998;38:2949–62.

49. Chung STL, Jarvis SH, Cheung S-H. The Effect of Dioptric Blur on Reading Performance. Vision Res 2007;47:1584–94.

50. Khuu SK, Chou PH, Ormsby J, Kalloniatis M. The Effect of Optical Blur on Central and Peripheral Word Visual Acuity. Optom Vis Sci 2013;90:1443–9.

51. Ramulu PY, Swenor BK, Jefferys JL, Friedman DS, Rubin GS. Difficulty with Out-Loud and Silent Reading in Glaucoma. Invest Ophthalmol Vis Sci 2013;54:666–72.

52. Kwon M, Legge GE. Higher-contrast requirements for recognizing low-pass–filtered letters. J Vis 2013;13:13–13.

53. Tan JCK, Nguyen V, Fenwick E, Ferdi A, Dinh A, Watson SL. Vision-Related Quality of Life in Keratoconus: A Save Sight Keratoconus Registry Study. Cornea 2019;38:600–4.

54. Kandel H, Pesudovs K, Watson SL. Measurement of Quality of Life in Keratoconus. Cornea 2020;39:386–93.

55. Young LK, Liversedge SP, Love GD, Myers RM, Smithson HE. Not all aberrations are equal: reading impairment depends on aberration type and magnitude. J Vis 2011;11:20.

56. Sabesan R, Yoon G. Neural Compensation for Long-term Asymmetric Optical Blur to Improve Visual Performance in Keratoconic Eyes. Invest Ophthalmol Vis Sci 2010;51:3835–9.

57. Sabesan R, Barbot A, Yoon G. Enhanced neural function in highly aberrated eyes following perceptual learning with adaptive optics. Vision Res 2017;132:78–84.

58. Carkeet A. Modeling logMAR visual acuity scores: effects of termination rules and alternative forced-choice options. Optom Vis Sci 2001;78:529–38.

59. Rajpurkar P, Zhang J, Lopyrev K, Liang P. SQuAD: 100,000+ Questions for Machine Comprehension of Text. ArXiv160605250 Cs October 2016.

60. Prahalad KS, Coates DR. Asymmetries of reading eye movements in simulated central vision loss. Vision Res 2020;171:1–10.

61. Prins N, Kingdom FAA. Applying the Model-Comparison Approach to Test Specific Research Hypotheses in Psychophysical Research Using the Palamedes Toolbox. Front Psychol 2018;9.

62. Wagner H, Barr JT, Zadnik K. Collaborative Longitudinal Evaluation of Keratoconus (CLEK) Study: Methods and Findings to Date. Cont Lens Anterior Eye 2007;30:223–32.

63. Brysbaert M. How many words do we read per minute? A review and meta-analysis of reading rate. J Mem Lang 2019;109:104047.

64. Ginsburg AP. Contrast Sensitivity and Functional Vision. Int Ophthalmol Clin 2003;43:5–15.

65. Mannis MJ, Ling JJ, Kyrillos R, Barnett M. Keratoconus and Personality-A Review. Cornea 2018;37:400–4.

66. Bradley A, Thomas T, Kalaher M, Hoerres M. Effects of Spherical and Astigmatic Defocus on Acuity and Contrast Sensitivity: A Comparison of Three Clinical Charts. Optom Vis Sci 1991;68:418–26.

67. Ross JE, Bron AJ, Clarke DD. Contrast sensitivity and visual disability in chronic simple glaucoma. Br J Ophthalmol 1984;68:821–7.

68. Hawkins AS, Szlyk JP, Ardickas Z, Alexander KR, Wilensky JT. Comparison of Contrast Sensitivity, Visual Acuity, and Humphrey Visual Field Testing in Patients with Glaucoma. J Glaucoma 2003;12:134–8.

69. Hyvärinen L, Laurinen P, Rovamo J. Contrast Sensitivity in Evaluation of Visual Impairment Due to Diabetes. Acta Ophthalmol (Copenh) 1983;61:94–101.

70. Sokol S, Moskowitz A, Skarf B, Evans R, Molitch M, Senior B. Contrast Sensitivity in Diabetics With and Without Background Retinopathy. Arch Ophthalmol 1985;103:51–4.

71. Kleiner RC, Enger C, Alexander MF, Fine SL. Contrast Sensitivity in Age-Related Macular Degeneration. Arch Ophthalmol 1988;106:55–7.

72. Stangos N, Voutas S, Topouzis F, Karampatakis V. Contrast Sensitivity Evaluation in Eyes Predisposed to Age-Related Macular Degeneration and Presenting Normal Visual Acuity. Ophthalmologica 1995;209:194–8.

73. Bradley A, Freeman RD. Contrast sensitivity in anisometropic amblyopia. Invest Ophthalmol Vis Sci 1981;21:467–76.

74. Li J, Spiegel DP, Hess RF, Chen Z, Chan LYL, Deng D, Yu M, Thompson B. Dichoptic training improves contrast sensitivity in adults with amblyopia. Vision Res 2015;114:161–72.

75. Mai ELC, Lian I-B, Chang DCK. Assessment of contrast sensitivity loss after intrastromal femtosecond laser and LASIK procedure. Int J Ophthalmol 2016;9:1798–801.

76. Pelli DG, Robson JG, J AJW. The design of a new letter chart for measuring contrast sensitivity. Clin Vis Sci 1988:187–99.

77. Dougherty BE, Flom RE, Bullimore MA. An Evaluation of the Mars Letter Contrast Sensitivity Test. Optom Vis Sci 2005;82:970–5.

78. Rodríguez-Vallejo M, Remón L, Monsoriu JA, Furlan WD. Designing a new test for contrast sensitivity function measurement with iPad. J Optom 2015;8:101–8.

79. Bullimore M, Jansen M, Kollbaum E, Kollbaum P. An iPad Test of Letter Contrast Sensitivity. Invest Ophthalmol Vis Sci 2013;54:5331–5331.

80. Mäntyjärvi M, Laitinen T. Normal values for the Pelli-Robson contrast sensitivity test11None of the authors has a financial or proprietary interest in any material or method mentioned. J Cataract Refract Surg 2001;27:261–6.

81. Haymes SA, Chen J. Reliability and Validity of the Melbourne Edge Test and High/Low Contrast Visual Acuity Chart: Optom Vis Sci 2004;81:308–16.

82. Thayaparan K, Crossland MD, Rubin GS. Clinical assessment of two new contrast sensitivity charts. Br J Ophthalmol 2007;91:749–52.

83. Robson J, Sapotka R, Kidd J, Newman D, Pardhan S. Self-assessment of visual function using new single-use printed charts. Invest Ophthalmol Vis Sci 2016;57.

84. Griffin A, Cheng H, Robson J. Measuring Contrast Sensitivity using CambBlobs2 Disposable Paper Charts in Normal Subjects. Invest Ophthalmol Vis Sci 2017;58:4231–4231.

85. Robson J, Raman R, Srinivasan R, Pardhan S. Contrast sensitivity in glaucoma using simple disposable printed (CamBlobs) charts. Invest Ophthalmol Vis Sci 2019;60:2488–2488.

86. Blackwell HR. Contrast Thresholds of the Human Eye. J Opt Soc Am Opt Image Sci Vis 1946;36:624–43.

87. Thibos LN, Applegate RA, Schwiegerling JT, Webb R, VSIA Standards Taskforce Members. Standards for Reporting the Optical Aberrations of Eyes. In: Vision Science and Its Applications. Vol Santa Fe, New Mexico: J Opt Soc Am A Opt Image Sci Vis; 2000:SuC1.

88. Elliott DB, Sanderson K, Conkey A. The reliability of the Pelli-Robson contrast sensitivity chart. Ophthalmic Physiol Opt 1990;10:21–4.

89. Tchakmakian L, Bachir V, Wittich W, Marinier J-A. Camblobs2™, a novel chart for contrast sensitivity testing, shows correlation to Mars™ chart in MS patients with optic neuritis. Invest Ophthalmol Vis Sci 2019;60:2281–2281.

90. Bland JM, Altman DG. Statistical methods for assessing agreement between two methods of clinical measurement. Lancet 1986;1:307–10.

91. West SK, Rubin GS, Broman AT, Muñoz B, Bandeen-Roche K, Turano K, for the SEE Project Team. How Does Visual Impairment Affect Performance on Tasks of Everyday Life?: The SEE Project. Arch Ophthalmol 2002;120:774–80.

92. Aydin Kurna S, Altun A, Gencaga T, Akkaya S, Sengor T. Vision Related Quality of Life in Patients with Keratoconus. J Ophthalmol 2014;2014.

93. Ravikumar A, Applegate RA, Shi Y, Bedell HE. Six just-noticeable differences in retinal image quality in 1 line of visual acuity: Toward quantification of happy versus unhappy patients with 20/20 acuity. J Cataract Refract Surg 2011;37:1523–9.